AD-A120 879 FUEL PROPERTY EFFECTS ON DIESEL ENGINE AND GAS TURBINE COMBUSTOR PERFORMANCE(U) SOUTHWEST RESEARCH INST SAN ANTONIO TX A F MONTEMAYOR ET AL. NOV 81 1/1

UNCLASSIFIED SWRI-6800-120/1 DAAK70-80-C-0001 F/G 21/2 NL

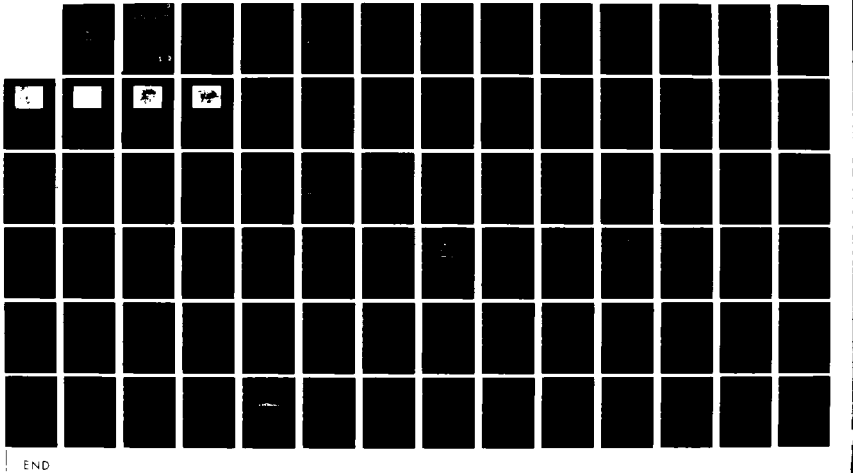

END

FILMED

DTIC

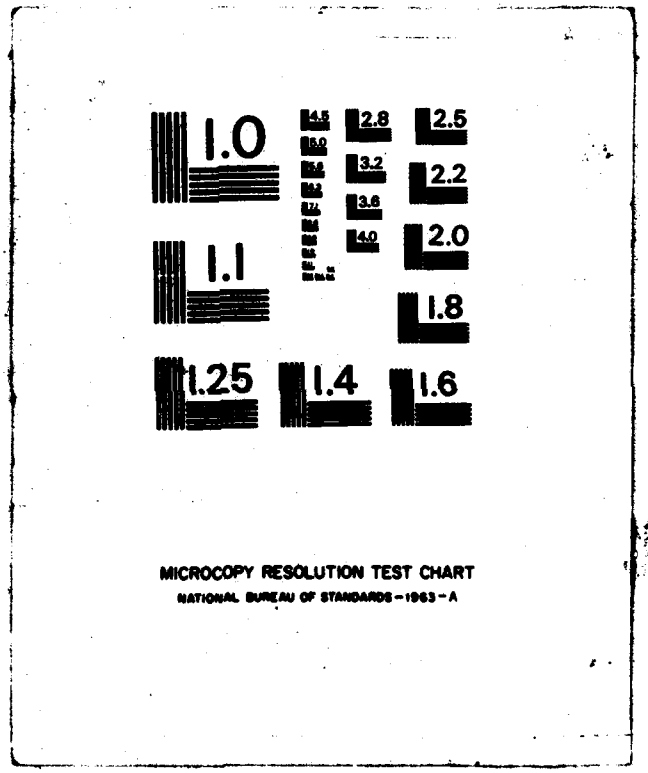
1.0
4.5
5.0
2.8
3.2
3.6
4.0
2.5
2.2
2.0
1.8
1.1
1.25
1.4
1.6
MICROCOPY RESOLUTION TEST CHART
NATIONAL BUREAU OF STANDARDS-1963-A

AD A 120879

12

FUEL PROPERTY EFFECTS ON DIESEL ENGINE AND GAS TURBINE COMBUSTOR PERFORMANCE

INTERIM REPORT
AFLRL No. 149

By

A.F. Montemayor
D.W. Naegeli
L.G. Dodge
E.C. Owens
J.N. Bowden
U.S. Army Fuels and Lubricants Research Laboratory
Southwest Research Institute
San Antonio, Texas

Under Contract to

U.S. Army Mobility Equipment Research and Development Command
Energy and Water Resources Laboratory
Fort Belvoir, Virginia

Contract No. DAAK70-82-C-0001

DTIC FILE COPY

DTIC ELECTE NOV 0 1 1982 S D E

Approved for public release; distribution unlimited

December 1981

82 11 01 082

Disclaimers

The findings in this report are not to be construed as an official Department of the Army position unless so designated by other authorized documents.

Trade names cited in this report do not constitute an official endorsement or approval of the use of such commercial hardware or software.

DTIC Availability Notice

Qualified requestors may obtain copies of this report from the Defense Technical Information Center, Cameron Station, Alexandria, Virginia 22314.

Disposition Instructions

Destroy this report when no longer needed. Do not return it to the originator.

UNCLASSIFIED

SECURITY CLASSIFICATION OF THIS PAGE *(When Data Entered)*

REPORT DOCUMENTATION PAGE

READ INSTRUCTIONS BEFORE COMPLETING FORM

1. REPORT NUMBER: AFLRL NO. 149

2. GOVT ACCESSION NO.: AD-A120879

3. RECIPIENT'S CATALOG NUMBER:

4. TITLE *(and Subtitle)*: FUEL PROPERTY EFFECTS ON DIESEL AND GAS TURBINE COMBUSTOR PERFORMANCE

5. TYPE OF REPORT & PERIOD COVERED: Interim Report Oct 1980 - Dec 1981

6. PERFORMING ORG. REPORT NUMBER: SwRI-6800-120/1

7. AUTHOR(s): A.F. Montemayor, D.W. Naegeli, L.G. Dodge, E.C. Owens, J.N. Bowden

8. CONTRACT OR GRANT NUMBER(s): DAAK70-80-C-0001, DAAK70-82-C-0001

9. PERFORMING ORGANIZATION NAME AND ADDRESSES: U.S. Army Fuels and Lubricants Research Lab, Southwest Research Institute, P.O. Drawer 28510, San Antonio, TX 78284

10. PROGRAM ELEMENT, PROJECT, TASK AREA & WORK UNIT NUMBERS: 1L762733AH20EH; WUB03

11. CONTROLLING OFFICE NAME AND ADDRESS: U.S. Army Mobility Equipment Research and Development Command, Energy and Water Resources Lab. Fort Belvoir, VA 22060

12. REPORT DATE: November 1981

13. NUMBER OF PAGES: 75

14. MONITORING AGENCY NAME & ADDRESS *(if different from Controlling Office)*:

15. SECURITY CLASS. *(of this report)*: Unclassified

15a. DECLASSIFICATION/DOWNGRADING SCHEDULE:

16. DISTRIBUTION STATEMENT *(of this Report)*

Approved for public release; distribution unlimited

17. DISTRIBUTION STATEMENT *(of the abstract entered in Block 20, if different from Report)*

18. SUPPLEMENTARY NOTES

19. KEY WORDS *(Continue on reverse side if necessary and identify by block number)*

Fuel Requirements	Fuel Properties	Energy
Cetane	Load	Regression
Viscosity	Diesel Engines	Statistical
Boiling Point	Army Engines	Analysis
Aromatic Content	Speed	Fuel Blends

20. ABSTRACT *(Continue on reverse side if necessary and identify by block number)*

In this test program, four military engines and a gas turbine combustor were run to determine the effects of fuel properties on combustion performance. During this program, 18 test fuels were prepared with properties extending beyond the range of the specifications of diesel fuels. Diesel engine performance data were analyzed statistically, and regression equations were obtained for each engine expressing load in terms of speed, energy input,

DD FORM 1 JAN 73 1473 EDITION OF 1 NOV 65 IS OBSOLETE

UNCLASSIFIED

SECURITY CLASSIFICATION OF THIS PAGE *(When Data Entered)*

20. ABSTRACT (continued)

cetane number, kinematic viscosity, 10-percent boiling point, and aromatic content. Combustion performance measurements in the T-63 gas turbine combustor included flame radiation, exhaust smoke, gaseous emissions (THC, CO and NO_x), combustion efficiency, and ignition properties. The atomizing characteristics of the test fuels were examined with a particle sizing system based on forward-angle diffraction, and the results were correlated with the ignition properties of the fuels. Flame radiation and exhaust smoke were correlated with H/C ratio of the fuel. Viscosity and end point work were used as correlating parameters for THC and CO emissions, and combustion efficiency. Significance of the results was discussed, and recommendations for further testing was presented.

Accession For
NTIS GRA&I
DTIC TAB
Unannounced
Justification
By
Distribution/
Availability Codes
Dist | Avail and/or Special
A

DTIC COPY INSPECTED

SUMMARY

Four military engines were tested to determine the effect of fuel properties on engine performance. These engines were the Detroit Diesel (DD) 4-53T, Continental Motors LDT-465-1C, Cummins NTC-350, and the Caterpillar 3208T. For this program, 18 fuels were blended to attain wide variations in kinematic viscosity, cetane number, ten-percent boiling point (10%BP), and aromatic content. Each of the eighteen fuels was run at the same relative speed and energy levels in each engine. Loads attained from the given speed-energy points were analyzed using the computer program BMDP1R. These multiple linear regression analyses yielded a stable load prediction equation for each engine with energy, speed, aromatic content, kinematic viscosity, and 10%BP as the independent variables. Two additional fuel blends were run as cross-validations. Predicted loads agreed well with observed loads for these fuels except at low speed-energy points in some engines.

The performance of the 4-53T engine was adversely affected by highly aromatic fuels. The performance of the LDT-465-1C engine was adversely affected by low 10%BP fuels. Neither the NTC-350 or the 3208T engines were significantly affected by changes in fuel properties over the ranges tested. In general, the 3208T engine produced the highest load per unit of energy input, primarily because the engine was derated due to miscalibration of the injection system by the manufacturer. The 3208T engine was operated significantly below its rated power, and results obtained in this report should be considered a subset of total engine performance. This series of tests did not address maximum power availability, cold weather operation, or long-term operational problems that could arise from operation of these engines on off-specification fuels.

Combustion performance measurements were made in a T-63 gas turbine combustor at operating conditions of idle, cruise, climb, and takeoff. Ignition measurements were made at air flow conditions typical for the T-63 engine; the tests were made with room temperature (25°C) air. Combustion performance measurements on eighteen test fuels and two referee fuels included flame radiation, exhaust smoke, gaseous emissions (THC, CO, and NO_x),

and combustion efficiency. The exhaust smoke and flame radiation measurements for the eighteen test fuels at the takeoff condition correlated favorably with H/C ratio. Correlations based on multiple linear regression analyses of total hydrocarbons (THC), CO emission, and combustion efficiency at the idle condition with fuel viscosity and end point were poor; nevertheless, they predicted trends in the two referee fuels and agreed with theory. The regression analysis indicated that viscosity was a more important property in determining gaseous emissions of THC and CO than the end point. However, this indication was somewhat tenuous because there was a strong correlation of viscosity with end point in the test fuels. The NO_x emissions were essentially independent of the fuel properties. None of the fuels contained significant amounts of nitrogen, so NO_x was formed principally from the nitrogen in the air.

The spray quality of the T-63 nozzle was measured at ignition conditions. A forward laser light-scattering instrument was used to measure the Rosin-Rammler parameters at one location in the spray. A multiple variable regression analysis was used to predict the Sauter mean diameter of the droplets as a function of fuel properties and fuel pressure.

Ignition data for the T-63 combustor were correlated with fuel properties and droplet size.

FOREWORD

This work was conducted at the U.S. Army Fuels and Lubricants Research Laboratory (USAFLRL) located at Southwest Research Institute (SwRI), San Antonio, TX, under Contract Nos. DAAK70-80-C-0001 and DAAK70-82-C-0001 during the period October 1980 through December 1981. The work was funded by the U.S. Army Mobility Equipment Research and Development Command (USAMERADCOM), Ft. Belvoir, VA, with Mr. F.W. Schaekel (DRDME-GL) as the contracting officer's representative and Mr. M.E. LePera, Chief of Fuels and Lubricants Division (DRDME-GL), as the project technical monitor.

ACKNOWLEDGMENT

The authors wish to thank Dr. Robert Mason of Southwest Research Institute for his aid in conducting the statistical analysis presented herein. The assistance of Drs. T.W. Ryan and J. Erwin in developing fuel blending methodology and initial test matrix design is also gratefully acknowledged. The authors would like to acknowledge the assistance provided by the AFLRL technical and laboratory staff in the performance of the work and the AFLRL technical publications group in the preparation of this report. Special recognition is made of Messrs. K.E. Hinton and L.D. Sievers, chemical/analytical laboratory and engine laboratory supervisors, respectively.

TABLE OF CONTENTS

LIST OF TABLES

LIST OF ILLUSTRATIONS

I. INTRODUCTION

Due to the tightening world oil supply, the Army wishes to develop its capability to utilize multisource mobility fuels. As the sources of these fuels change, the basic properties of the fuels will also change. The Army currently specifies acceptable property limits for its fuels, but future economical considerations may necessitate expansion of these time-proven limits.

Qualitative fuel property effects on engine performance have long been known and have been incorporated into existing specification limits. Expansion of these limits requires quantitative knowledge of these fuel property effects in order to minimize performance degradation of Army vehicles.(1-3)* Figure 1 illustrates the process for evaluating new/synthetic fuels to assure that there will be no impairment to overall Army mission.(4) This work falls under the heading of Full-Scale Multicylinder Engine Performance Testing and basically provides feedback information to the qualification system.

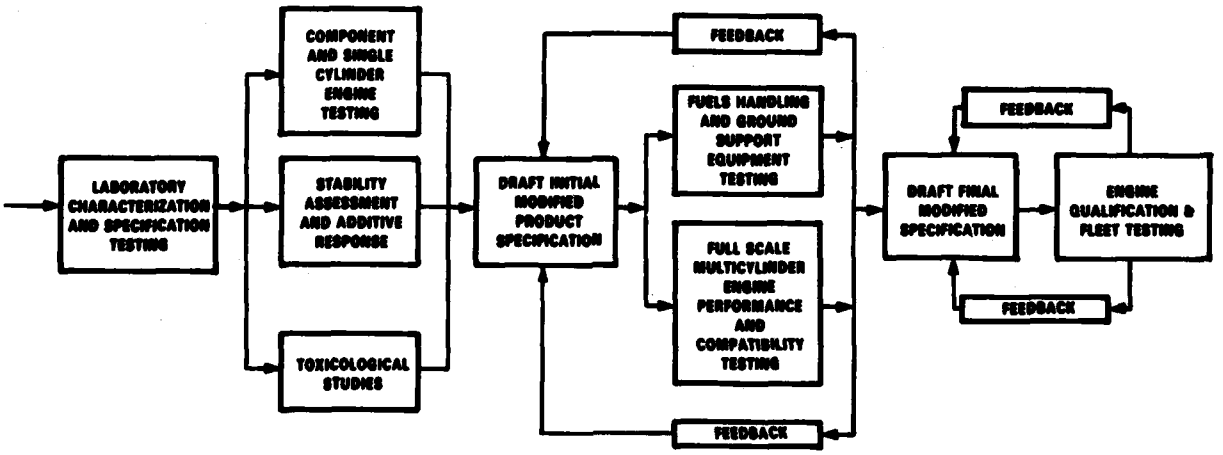

FIGURE 1. PROCESS FOR EVALUATING NEW/SYNTHETIC FUELS

* Underscored numbers in parentheses refer to the list of references at the end of this report.

For this study, four compression ignition (CI) engines were chosen because of their diverse fuel injection/combustion systems and their widespread use (or potential use) in Army tactical vehicles. Spark ignition (SI) engines were not included due to the predominance of CI engines in the Army tactical inventory and potential phaseout of SI engines. The four engines used were the Continental Motors LDT-465-1C, Detroit Diesel (DD) 4-53T, Cummins NTC-350, and the Caterpillar 3208T. Test setups and engine specifications for the engines are shown in Figures 2 through 5, respectively.

Fuel properties affecting diesel engine performance are heat of combustion, viscosity, volatility, cetane number, and aromatic content. Heat of combustion is a measure of how much energy the combustion of a given amount of fuel will produce. The net heat of combustion (accounting for water in the combustion byproducts) was used throughout this report in order to quantify the amount of energy introduced into the combustion process. Fuel viscosity affects atomization and penetration of the fuel into the combustion chamber. This, in turn, affects combustion due to changes in fuel surface area and charge placement. Throughout this report, kinematic viscosity at 40°C is used as a measure of fuel viscosity. Fuel volatility affects the vaporization of fuel and thus affects combustion. ASTM D 86 percent recovered temperatures are a convenient way to measure volatility and are used throughout this report. Cetane number is a measure of ignition delay. This affects performance by releasing the fuel's energy earlier or later in the cycle. Aromatic content is a measure of the percentage of ringed carbon molecules in a fuel. Since aromatics generally ignite poorly under compression ignition, the percentage of aromatics should generally affect engine performance.

Fuels utilized in these tests are listed and discussed in Section II of this report. Cat 1-H/1-G reference diesel fuel was selected as the base fuel due to its batch-to-batch uniformity and general acceptance as a base fuel. Other fuels utilized were chosen or blended on site to obtain a wide range of fuel properties.

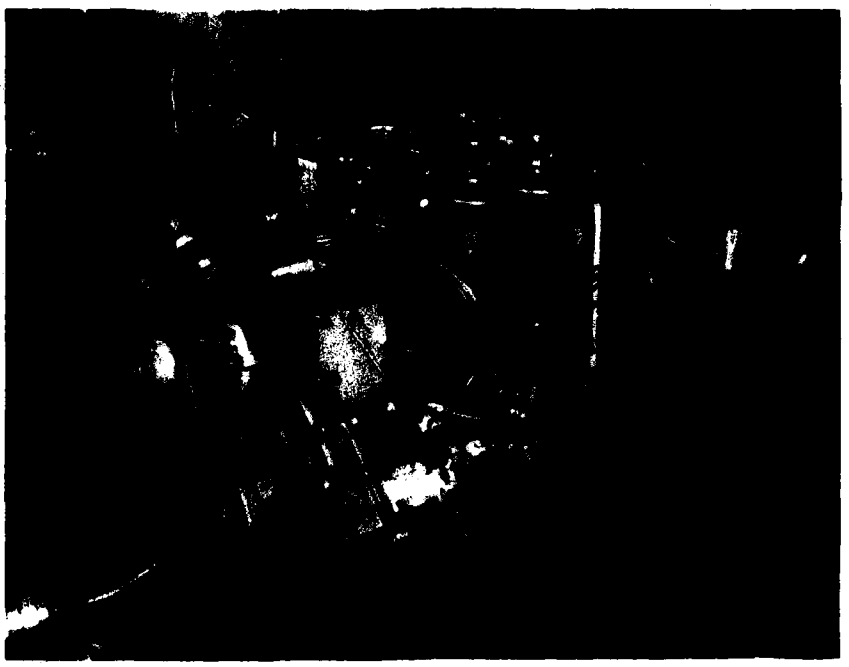

Model: LDT-465-1C
Engine Type: Four-cycle compression ignition, M.A.N. combustion system, turbocharged
Cylinders: 6, inline
Displacement: 7.83 L (478 $in.^3$)
Bore: 11.58 cm (4.56 in.)
Stroke: 12.37 cm (4.87 in.)
Compression Ratio: 22:1
Fuel Injection: Bosch Rotary Distributor w/Density Compensation
Rated Power: 145-156 kW (194-209 BHP) at 2800 RPM
Rated Torque: 597 N·M (429 lb-ft) at 2000 RPM

FIGURE 2. CONTINENTAL MOTORS LDT-465-1C TEST SETUP AND ENGINE SPECIFICATIONS

Model: 4-53T(5047-5340)
Engine Type: Two-cycle compression ignition, direct injection, uniflo scavenging, turbosupercharged
Cylinders: 4, inline
Displacement: 3.48 L (212 $in.^3$)
Bore: 9.84 cm (3.87 in.)
Stroke: 11.43 cm (4.5 in.)
Compression Ratio: 18.7:1
Fuel Injection: DD 5A60 unit injectors
Rated Power: 127 kW (170 BHP) at 2500 RPM
Rated Torque: 545 N M (402 lb-ft) at 1800 RPM

FIGURE 3. DETROIT DIESEL 4-53T TEST SETUP AND ENGINE SPECIFICATIONS

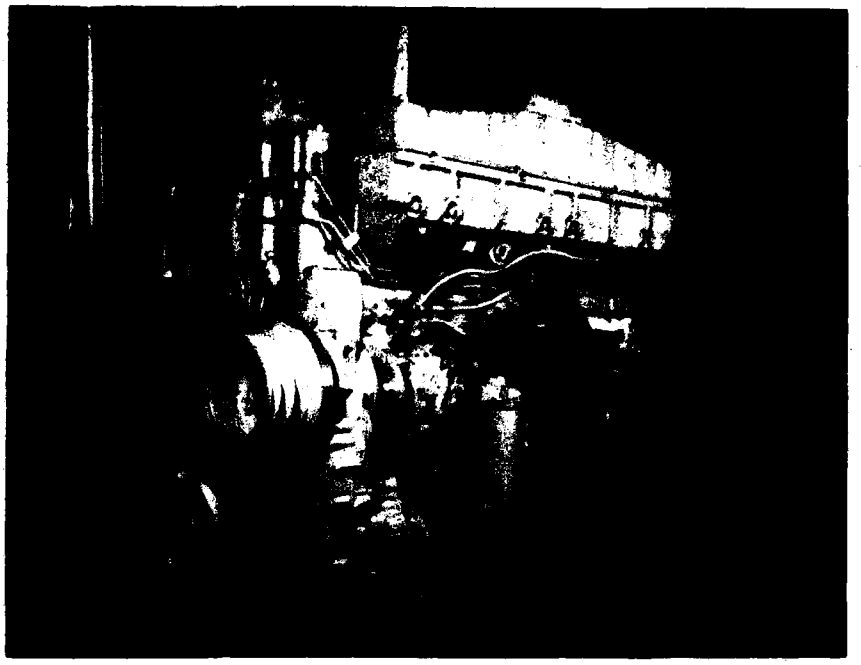

Model: NTC-350
Engine Type: Four-cycle compression ignition, direct injection
Cylinders: 6, inline
Displacement: 14.01 L (855 $in.^3$)
Bore: 13.97 cm (5.5 in.)
Stroke: 15.24 cm (6 in.)
Compression Ratio: 14.5:1
Fuel Injection: Cummins pressure-time
Rated Power: 261 kW (350 BHP) at 2100 RPM
Rated Torque: 1519 N·M (1120 lb-ft) at 1300 RPM

FIGURE 4. CUMMINS NTC-350 TEST SETUP AND ENGINE SPECIFICATIONS

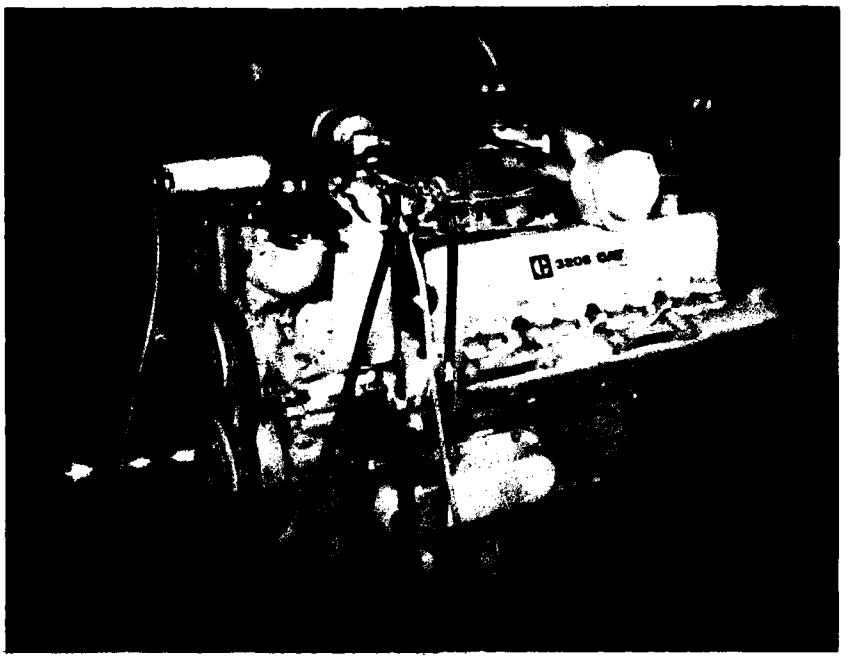

Model: 3208T
Engine Type: Four-cycle compression ignition, direct injection
Cylinders: 8, V configuration
Displacement: 10.42 L (636 $in.^3$)
Bore: 11.43 cm (4.5 in.)
Stroke: 12.70 cm (5 in.)
Compression Ratio: 16.5:1
Fuel Injection: Caterpillar scroll system
Rated Power: 224 kW (300 BHP) at 2800 RPM

Note: Engine would not attain 300 BHP due to factory misadjustment of fuel system. Test was run under derated conditions.

FIGURE 5. CATERPILLAR 3208T TEST SETUP AND ENGINE SPECIFICATIONS

Several recent studies (5-9) have been conducted to determine the properties of gas turbine fuel that will allow adequate fuel availability, but will also avoid sacrifices in engine performance and environmental acceptability. All engines now in production or under development were designed for satisfactory performance and life on the current specifications for petroleum distillate fuels. Many engines may not be able to tolerate the changes implied by a broader fuel specification, e.g., higher liner temperatures or longer droplet lifetimes. Operation on other fuels may or may not lead to a reduction in performance or increased maintenance requirements; however, at present there is a general lack of knowledge on fundamental relationships between fuel composition, properties, and performance, making a prior judgment on the acceptability of nonspecification fuels somewhat tenuous.

Among the properties of greatest concern to gas turbine combustion performance are fuel composition, distillation curve, and viscosity. The first property is generally associated with flame radiation and exhaust smoke; the latter two affect atomization and vaporization, and therefore, affect ignition, gaseous emissions, combustion efficiency, and flame stabilization. Because of the additional NO_x found in the exhaust, fuel-bound nitrogen is one new fuel property which has emerged from the use of syncrude fuels, primarily shale oil.

The fuels described in Section II of this report express a significant variation in the fuel properties that affect soot formation, gaseous emissions, combustion efficiency, and ignition properties. In this work, combustion performance measurements on the test fuels are made in a T-63 gas turbine combustor at the operating conditions, idle, cruise, climb, and takeoff. Ignition studies were performed at typical flow conditions with room temperature air.

II. SELECTION OF FUELS FOR TESTING

An objective of this testing program was to assess the effects of a variation in individual fuel property on engine performance, independent of

other fuel properties. This information is of interest since it can be used to evaluate and set fuel specification limits to maximize fuel availability without adversely impacting engine power or fuel consumption. The difficulty is that it is virtually impossible to vary one fuel property of interest without changing other properties as well. Thus, some method of analysis must be used which will account or compensate for the effect of these unintentional fuel property changes. The usual approach is to conduct a regression analysis which attempts to account for the observed data by minimizing the error between the observed data and the predictions of a "model" describing the engine response. In this project, the prediction model used was that each fuel variable of interest affected engine performance in a linear fashion. The model also accounted for engine speed and fuel input rate.

The fuel properties of interest in this program were kinematic viscosity at 40°C, cetane number, volatility, and aromatic content. Both the ASTM D 86 10 percent recovered temperature and the average of the 10, 50, and 90 percent recovered temperatures were used as measures of volatility.

The ability of the regression analysis to predict accurately the dependent variable being modeled is determined by the accuracy of the measurements, the range of values that the independent variables span, and the number of data points. The accuracy of measurements is generally equipment-dependent, and the property value range is a function of the design of the test. Therefore, the primary test design variable which can be controlled is the number of data points. Unfortunately, increasing the number of test points also increases test cost. As a result, the number of points must be a balance between cost and prediction accuracy. With this in mind, an analysis was conducted to estimate the number of fuel test points required. This analysis, detailed in Appendix A, indicated that a minimum of 16 fuel blends would be required for a reasonable analysis. As a result, 18 test blends were selected.

After the number of fuel blends was determined, the next objective was to select the composition of the blends to maximize the information obtained.

The initial approach to specifying the test fuel compositions was to use a commercial computerized experiment design program called Computer Optimized Experimental Design (COED).

It became apparent that this approach would not provide sufficient fuel guidance. However, since COED placed points in the corners of the specified property space, producible fuel blends were chosen with properties as close to the corners of the property space as possible. To establish these blends, a program was developed to estimate the properties of a fuel blend given the properties of the blend stocks. Briefly, the program required that the relationship between the blendstock concentration and the resulting fuel composition be linear. This required that methods be found to describe the blending of the fuel properties of interest in a linear fashion.

The aromatics may be treated directly by averaging the percent aromatics in each blend component multiplied by its volume fraction (f_i) in the mixture. Also, an initial stage of the work using practice blends revealed that kinematic viscosity using a Viscosity Blending Index Factor (VF) is treated satisfactorily. For kinematic viscosity, the viscosity of the blend is

$$VF_{blend} = \sum_i f_i \, VF_i$$

and it would be convenient to work with VF.

The volatility offered more resistance to prediction. It is most appropriately expressed as moles evaporated at several fixed temperatures. Averaging these moles of blendstock at fixed temperature was the most feasible method of determining volatility. Employing an ASTM Method D 86-type measure (T at fixed volume reductions) in the trial formulations, averaging temperatures at 10 percent evaporated and 10, 50, 90 percent, as well as averaging volume off at three fixed temperatures, were checked. Though the method of averaging temperatures is least like the "mole method," better agreement was obtained. With this approach, approximately 7 percent deviation between calculated and measured volatility was observed.

The cetane number characterization required the most effort. The trial predictions showed notable nonlinearities in blends of high and low cetane fuels. To quantify these effects, nine blends of seven actual stocks were made for measuring cetane number (CN). The matrix of points was selected to determine nonlinearities in the most efficient way.

The results from this investigation were regressed, yielding:

$$CN = 11.44 + 5.562\ F_1 - 16.42\ F_2 + 31.38\ F_3 + 33.29\ F_4 + 16.42\ F_2^2 - 13.73\ F_3^2 + 7.697\ F_4^2$$

where F_1 = fraction of High Aromatic Naphtha (HAN)(AL-10223-F) in the mixture

F_2 = fraction of Benzene Toluene Xylene (BTX) Bottoms (AL-10233-F) in the mixture

F_3 = fraction of JP-4 (AL-9254) in the mixture

F_4 = fraction of CAT 1-H (AL-10433) in the mixture

This function is only valid for F_1 if $F_2 = 0$ and conversely.

Many plots of this function show that HAN will blend closely enough to linear at all combinations of high and middle components, so that its cetane number may be used directly.

Heavy BTX bottoms do well with the middle-cetane stock, but induce marked curvature when the other component has appreciable high-cetane stock in it.

After completion, this program was able to reasonably estimate the properties of any given combination of our blending components. This program was then used to generate a large list (>5000) of potential fuel properties. From this list, fuels were selected which had properties within the ranges of interest.

Table 1 shows the volume percentage of the blendstocks in each of the 18 fuels in the test matrix. The first three fuels in the matrix were Cat 1-H,

JP-4, and Jet A. Table 2 lists predicted properties of the 18 test fuels compared to the measured properties of the final fuels and blends. The predicted values were based on the selected properties for the blending stocks listed in Table 3. The properties of the blending stocks are listed in Table 4, and include the base fuels (Test Fuels 1, 2, and 3). The properties of the final test fuel blends (Test Fuels 4 through 18) are shown in Table 5.

Since the engines undergoing evaluation were designed for using DF-2 as the primary fuel, the properties of the 18 test fuels were compared to Federal Specification VV-F-800C, Fuel Oil, Diesel, shown in Table 6.

This Federal specification permits a maximum temperature of 338°C at 90 percent evaporated in the ASTM Method D 86 distillation test for grade DF-2. Fourteen test fuels fell below the maximum allowed, and 13 were below the end point requirement of 370°C maximum. The lowest 90 percent evaporated temperature for the test fuels was 217°C and the highest was 367°C. End points for the test fuels ranged from 253°C to 398°C.

VV-F-800C allows a range of 1.9 to 4.1 cSt, kinematic viscosity at 40°C for DF-2. Of the test fuels, nine fell within these limits; eight had viscosities within the DF-1 limits; eleven met DF-A viscosity requirements; and two fuels had viscosities below 1.1 cSt of the DF-A minimum requirement. The lowest test fuel viscosity was 0.78 cSt and the highest was 3.55 cSt.

In addition, eight test fuels had cetane numbers above 45, the minimum value shown for DF-1 and DF-2 in the federal specification; four test fuels had cetane numbers between 40 and 45, and six were below 40. At present, a cetane number of 40 is permitted for DF-1 and DF-2 fuels. The lowest cetane number for the test fuels was 31.3 and the highest was 53.1.

Aromatic content is not a specification requirement; however, it is a property considered to be influential in the combustion event and was included in the design of the test fuel matrix. The aromatics in these test fuels ranged from 12.9 to 61.9 vol%, as measured by the ASTM D 1319 Fluorescent Indicator Absorption (FIA) Test.

TABLE 1. COMPOSITION OF TEST FUELS BY VOLUME PERCENT

AL No.	Test Fuel No.	Cat 1-H AL-10697-F	Jet A AL-10582-F	JP-4 AL-10583-T	Hvy BTX Bottoms AL-10716-A	Kerosene AL-10724-F	Hvy Arom. Naphtha AL-10735-A	Gas Oil AL-10849-F
10697-F	1	100	---	---	---	---	---	---
10583-T	2	---	---	100	---	---	---	---
10582-T	3	---	100	---	---	---	---	---
10854-F	4	80.8	3.2	3.2	3.2	3.2	3.2	3.2
10855-F	5	85	---	---	15	---	---	---
10856-F	6	---	---	20	---	80	---	---
10754-F	7	40	60	---	---	---	---	---
10857-F	8	---	---	45	---	---	---	55
10858-F	9	---	45	---	---	---	---	55
10859-F	10	50	---	---	---	---	50	---
10710-F	11	55	---	45	---	---	---	---
10860-F	12	---	---	---	---	---	40	60
10711-F	13	---	70	30	---	---	---	---
10861-F	14	---	---	70	---	---	---	30
10862-F	15	---	70	---	30	---	---	---
10712-F	16	25	---	75	---	---	---	---
10863-F	17	---	80	---	20	---	---	---
10864-F	18	85	---	---	---	---	---	15

TABLE 2. SELECTED PROPERTIES OF 18 FUELS WHICH COMPRISE THE TEST MATRIX

Test	K. Viscosity at 40°C, cSt		ASTM D86 10%BP, °C		Avg. Boiling Temperature °C*		Cetane No.		Aromatic Content, %	
Fuel No.	Pred.**	Meas.***	Pred.	Meas.	Pred.	Meas.	Pred.	Meas.	Pred.	Meas.
1	3.2	3.2	241	238	276	277	53	50.1	28	31
2	0.71	0.78	90	91	140	156	28	34.5	9	15
3	1.0	1.5	172	195	185	216	50	44.5	13	17
4	2.5	2.56	231	203	264	262	50	47.5	30	34
5	2.5	2.33	234	193	264	225	46	42.9	38	42
6	1.5	1.16	172	159	195	191	52	46.1	8	13
7	1.5	1.98	200	201	221	242	51	46.4	19	24
8	1.9	2.19	198	113	248	251	44	48.1	15	24
9	2.5	3.33	236	209	268	283	54	50.1	17	28
10	2.0	2.07	219	204	294	249	35	32.0	56	59
11	1.4	1.63	173	116	215	221	42	45.4	20	22
12	3.2	3.49	251	214	291	289	41	39.8	45	62
13	0.92	1.21	148	144	172	194	43	40.8	12	17
14	1.1	1.30	149	103	199	218	37	41.7	12	18
15	0.97	1.14	178	176	189	200	37	31.3	38	43
16	0.92	1.04	128	99	174	188	34	38.3	14	18
17	1.0	1.25	177	181	188	210	42	34.5	29	35
18	3.5	3.55	248	241	285	286	54	53.1	27	31

* Average boiling temperature = $(\frac{10\% + 50\% + 90\%}{3})$°C by ASTM D 86.

** Predicted by blending correlations of the properties listed in Table 3.

*** Measured properties of test fuels with composition shown in Table 1.

TABLE 3. SELECTED PROPERTIES OF THE SEVEN BLENDING STOCKS

	JP-4	JET A	Cat 1-H	Gas Oil	High Aromatic Naphtha	Kerosene	Heavy BTX Bottoms
Kinematic Viscosity at 40°C, cSt	0.78	1.50	3.20	7.91	1.46	1.31	0.75
Viscosity Blending Index	0.123	0.247	0.350	0.442	0.240	0.224	0.114
10% BP, °C	91	195	238	293	194	186	161
$\frac{10+50+90\% \text{ Points}}{3}$, °C	156	216	277	336	222	200	164
Cetane No.	34.5	44.5	50.1	61.0	17.1	50.1	5.0
Aromatic Content, %	14.8	17.3	30.6	47.8	82.8	12.4	99.4

TABLE 4. PROPERTIES OF BASE FUELS AND BLENDING STOCKS

	AL-10697-F Cat 1-H Test Fuel 1	AL-10583-T JP-4 Test Fuel 2	AL-10582-F Jet A Test Fuel 3	AL-10716-A Heavy BTX Bottoms	AL-10724-F Kerosene	AL-10735-A Heavy Arom. Naphtha	AL-10849-F Gas Oil
Gravity, °API	34.6	54.0	42.2	31.1	46.5	27.1	33.1
Specific Gravity, g/mL	0.8519	0.8132	0.7628	0.8702	0.7949	0.8922	0.8597
Distillation, °C							
IBP	199	58	183	157	164	174	272
10% Recovered	238	91	195	161	186	194	293
50% Recovered	272	149	213	162	199	218	328
90% Recovered	322	229	241	169	216	253	*
EP	355	255	264	194	241	281	*
Residue, vol%	2.0	1.5	1.5	1.0	1.0	1.0	4.0
Loss, vol%	0	0	0	0	0	0	---
K. Viscosity, cSt at -20°C	Frozen	1.98	5.36	Frozen	4.23	5.86	Frozen
K. Viscosity, cSt at 40°C	3.20	0.78	1.50	0.75	1.31	1.46	7.91
Aromatics, FIA, vol%	30.6	14.8	17.3	99.4	12.4	82.8	47.8
Olefins, FIA, vol%	0.3	1.0	1.0	0.6	0.5	0.7	0
Mono-Aromatics, UV, wt%	6.85	10.60	9.59	52.50	5.20	35.05	4.92
Di-Aromatics, UV, wt%	7.82	1.19	1.31	1.70	3.10	11.31	4.08
Tri-Aromatics, UV, wt%	0.29	0.01	0.01	< 0.01	0.01	0.13	0.45
Hydrogen, wt%	13.03	14.34	13.81	10.07	14.17	10.91	13.24
Carbon, wt%	86.53	85.65	85.35	89.23	85.93	88.71	86.24
Nitrogen, wt%	0.01	< 0.01	<0.01	< 0.01	< 0.01	< 0.01	0.02
Sulfur, wt%	0.380	0.018	0.008	0	0	0.200	0.290
Refractive Index, 20°C	1.4751	1.4336	1.4512	1.4980	1.4429	1.5064	1.4783
Carbon Residue, 10% Btms, wt%	0.15	0.07	0.07	0.09	0.01	0.24	0.12
Aniline Point, °C(°F)	74(165)	57(135)	62(144)	-	-	-	96(205)
Flash Point, °C	74	-22	60	-	-	-	-
Net Heat of Combustion, MJ/kg	42.768	43.838	43.245	40.845	43.478	41.414	42.912
Btu/lb	18387	18847	18592	17560	18692	17805	18449
Calculated Net Heat of Combustion, MJ/kg	43.005	43.596	43.217	-	-	-	-
Btu/lb( )**	18489(9)	18743(9)	18580(7)	-	-	-	-
Cetane Number	50.1	34.5	44.5	5.0	50.1	17.1	61.0
Cetane Index (D 976-80)	47.7	34.7	43.9	0.8	46.4	21.4	52.4

* Boiling range too high for D 86.
** ASTM D 1405 Equation.

TABLE 5. PROPERTIES OF TEST FUEL BLENDS

	AL-10854-F Test Fuel 4	AL-10855-F Test Fuel 5	AL-10856-F Test Fuel 6	AL-10754-F Test Fuel 7	AL-10857-F Test Fuel 8	AL-10858-F Test Fuel 9	AL-10859-F Test Fuel 10
Gravity, °API	35.5	34.1	47.8	39.2	41.7	37.1	30.9
Specific Gravity, g/mL	0.8473	0.8545	0.7892	0.8294	0.8170	0.8393	0.8713
Distillation, °C							
IBP	132	163	94	174	71	189	173
10% Recovered	203	193	159	201	113	209	204
50% Recovered	266	266	198	230	278	273	242
90% Recovered	318	217	217	296	361	366	302
EP	353	349	253	330	395	398	341
Residue, vol%	1.0	1.5	1.0	1.5	2.0	2.0	1.5
Loss, vol%	1.0	0	0	0.5	1.0	0	0.5
K.Viscosity, cSt at -20°C	Frozen	Frozen	1.84	15.57	Frozen	Frozen	Frozen
K.Viscosity, cSt at 40°C	2.56	2.33	1.16	1.98	2.19	3.33	2.07
Aromatics, FIA, vol%	33.6	41.7	12.9	24.0	24.2	28.3	59.4
Olefins, FIA, vol%	1.5	1.6	0.9	1.2	0	1.1	1.3
Mono-Aromatics, UV, wt%	9.93	16.10	5.77	8.60	7.58	7.00	20.88
Di-Aromatics, UV, wt%	7.08	7.30	2.12	4.17	2.86	2.79	9.57
Tri-Aromatics, UV, wt%	0.27	0.26	0.03	0.12	0.28	0.27	0.21
Hydrogen, wt%	12.89	12.53	14.06	13.54	13.66	13.51	12.05
Carbon, wt%	86.09	86.71	85.64	86.43	85.84	86.28	87.80
Nitrogen, wt%	<0.01	<0.01	<0.01	<0.01	0.01	0.01	0.01
Sulfur, wt%	0.35	0.33	<0.001	0.16	0.17	0.16	0.29
Refractive Index, 20°C	1.4737	1.4788	1.4405	1.4600	1.4571	1.4660	1.4906
Carbon Residue, 10% Btms, wt%	0.11	0.10	0.07	0.10	0.11	0.11	0.12
Aniline Point, °C(°F)	62(144)	55(131)	64(147)	64(147)	73(163)	74(166)	35(95)
Flash Point, °C	45	57	12	64	<-5	73	65
Net Heat of Combustion, MJ/kg	42.522	42.265	43.019	43.243	42.349	42.554	41.963
Btu/lb	18281	18171	18495	18591	18207	18295	18041
Calculated Net Heat of Combustion, MJ/kg	42.978	42.815	43.466	43.143	43.336	43.245	42.426
Btu/lb( )*	18477(9)	18407(9)	18687(9)	18548(9)	18631(9)	18592(9)	18240(9)
Cetane Number	47.5	42.9	46.1	46.4	48.1	50.1	32.0
Cetane Index (D 976-80)	47.8	45.6	48.4	44.3	61.3	52.1	34.7

* ASTM D 1405 Equation.

TABLE 5. PROPERTIES OF TEST FUEL BLENDS (Cont'd)

	AL-10710-F Test Fuel 11	AL-10860-F Test Fuel 12	AL-10711-F Test Fuel 13	AL-10861-F Test Fuel 14	AL-10862-F Test Fuel 15	AL-10712-F Test Fuel 16	AL-10863-F Test Fuel 17	AL-10864-F Test Fuel 18
Gravity, °API	42.7	30.8	45.8	47.0	39.0	48.6	40.1	34.4
Specific Gravity, g/ml	0.8123	0.8718	0.7981	0.7927	0.8299	0.7857	0.8246	0.8529
Distillation, °C								
IBP	71	183	78	72	160	63	169	199
10% Recovered	116	214	144	103	176	99	181	241
50% Recovered	241	287	206	207	192	191	217	280
90% Recovered	305	367	233	345	231	275	233	337
EP	345	398	268	379	268	324	271	372
Residue, vol%	1.0	2.0	1.5	2.0	1.0	2.0	1.0	2.0
Loss, vol%	0	0	0	0	0	0	0	0
K. Viscosity, cSt at -20°C	11.40	Frozen	3.74	Frozen	Frozen	2.86	7.29	Frozen
K. Viscosity, cSt at 40°C	1.63	3.49	1.21	1.30	1.14	1.04	1.25	3.55
Aromatics, FIA, vol%	22.0	61.6	17.0	18.2	43.3	18.0	34.6	31.0
Olefins, FIA, vol%	0.5	3.0	0.5	0	1.2	0.7	1.1	0
Mono-Aromatics, UV, wt%	8.34	17.83	10.01	8.96	26.93	9.53	22.50	6.57
Di-Aromatics, UV, wt%	5.12	7.11	1.20	2.01	1.51	3.07	1.48	7.41
Tri-Aromatics, UV, wt%	0.20	0.31	0.01	0.14	0	0.08	0	0.35
Hydrogen, wt%	13.60	12.33	14.00	14.05	12.73	13.93	13.12	13.04
Carbon, wt%	86.21	87.43	86.08	86.06	87.17	86.64	86.72	86.44
Nitrogen, wt%	0.01	0.02	0.01	0.01	0.01	0.01	0.01	0.01
Sulfur, wt%	0.25	0.24	0.001	0.10	0.001	0.13	0.001	0.37
Refractive Index at 20°C	1.4569	1.4895	1.4450	1.4456	1.4649	1.4423	1.4601	1.4757
Carbon Residue, 10% Btms, wt%	0.04	0.11	0.07	0.10	0.05	0.11	0.06	0.10
Aniline Point, °C(°F)	62(144)	56(132)	60(140)	65(149)	36(96)	59(138)	45(113)	70(158)
Flash Point, °C	-11	73	2	-5	51	-23	52	75
Net Heat of Combustion, MJ/kg	43.147	41.959	43.578	43.001	42.246	43.393	42.561	42.503
Btu/lb	18550	18039	18735	18487	18163	18656	18298	18273
Calculated Net Heat of Combustion, MJ/kg	43.243	42.657	43.308	43.536	42.631	43.461	42.831	43.061
Btu/lb( )*	18591(9)	18363(9)	18619(9)	18717(7)	18328(9)	18685(7)	18414(9)	18513(9)
Cetane Number	45.4	39.8	40.8	41.7	31.3	38.3	34.5	53.1
Cetane Index (D 976-80)	54.3	44.3	47.8	50.9	29.3	47.0	34.8	48.9

* ASTM D 1405 Equation.

TABLE 6. PHYSICAL AND CHEMICAL REQUIREMENTS FOR FEDERAL SPECIFICATION VV-F-800C, FUEL OIL, DIESEL

Properties	Values			
			Grade DF-2	
	Grade DF-A	Grade DF-1	CONUS	OCONUS
Density, kg/L @ 15°C	Report	Report	Report	0.815 to 0.860
Flash point, °C min	38	38	52	56 (1)
Cloud point, °C max	-51	(2)	(2)	(2)
Pour point, °C max	Report	Report	Report	(3)
Kinematic viscosity @ 40°C, cSt	1.1 to 2.4	1.3 to 2.9	1.9 to 4.1	
Kinematic viscosity @ 20°C, cSt				1.8 to 9.5
Distillation, °C				
50% evaporated	Report	Report	Report	Report
90% evaporated, max	288	288	338	357
End point, max	300	330	370	370
Residue, vol%, max	3	3	3	3
Carbon residue on 10% bottoms, mass%, max (4)	0.10	0.15	0.35	0.20
Sulfur, mass%, max	0.25	0.50	0.50	0.70
Copper strip corrosion 3 hr @ 50°C, max rating	3	3	3	1
Ash, mass%, max	0.01	0.01	0.01	0.02
Accelerated stability, total insolubles, mg/100 ml, max (5)	1.5	1.5	1.5	1.5
Neutralization number TAN, max	0.05	---	---	0.10
Particulate contamination, mg/liter, max	10	10	10	10
Cetane number, min	40	45	45	45

(1) DF-2 intended for entry into the Central European Pipeline System shall have a minimum value of 58°C.
(2) As specified by the procuring activity of VV-F-800C.
(3) As specified by the procuring activity. DF-2 for Europe and S. Korea shall have a maximum limit of minus 18°C.
(4) See Appendix B of VV-F-800C. If the fuel contains cetane improvers, the test must be performed on the base fuel blend only.
(5) This requirement is applicable only for military bulk deliveries intended for tactical, OCONUS, or long-term storage (greater than six months) applications (i.e., Army depots, etc.).

III. DIESEL ENGINE TESTS

A. Test Matrix Design

The purpose of these tests was to determine the effects that fuel property changes would have on engine performance. Since these effects would be small, it was necessary to control factors that might mask fuel property effects. Speed, energy input, oil temperature, engine coolant temperature, inlet air temperature, humidity, and fuel temperature all affect the load that an engine produces. Speed and energy input are normally controlled by either a mechanical governor or, in the case of a vehicle, by a driver. Since most of the Army's engine applications are vehicular, it was determined that test matrix design should encompass normal speeds and loads found in vehicular applications (e.g., idle to full rack). Oil temperature, water outlet temperature, and fuel inlet temperature were all controlled in order to avoid masking fuel property effects. Inlet air temperature and humidity were not controlled due to lack of the required equipment. All engines were broken in according to manufacturers' recommended procedures.

The initial test matrix design incorporated four speeds with four energy levels each. In this report, energy input is expressed as Btu/injection and is generally calculated as:

$$\frac{\text{Btu}}{\text{injection}} = \frac{\text{Btu}}{\text{lb}} \times \frac{\text{lb}}{\text{hr}} \times \frac{\text{hr}}{60\ \text{min.}} \times \frac{\text{min.}}{\text{revolutions}} \times \frac{\text{revolution}}{\text{injection}}$$

Speeds were selected as 100, 75, 50, and 25 percent of full speed. Energy inputs varied from full rack to minimum flow at speed. Energy input was controlled so that corresponding points in different tests would be at the same energy level. It was hoped that this would emphasize fuel property effects rather than masking them with energy differences. A dynamometer controller controlled the speed, and an operator controlled the rack setting until the desired fuel flow (calculated from energy input) was achieved. Unfortunately, the 25-percent speed points proved to be destructive to the test apparatus. At these low speeds (slightly higher than idle), low-

frequency high-amplitude torsional vibrations between the engine and dynamometer severely damaged driveshafts. Because of this damage, the 25-percent speed points were dropped from the test matrix. Since a large number of engine runs were required by this test procedure, an in-house computer program was used to generate run sheets for the engines. Basically, the engine designation, test number, fuel number, fuel net heat of combustion, and engine operating data were processed into the program, and a run sheet was returned to the operator. To obtain the widest speed and fuel flow range (to simulate vehicular use), the program assumed 100, 75, and 50 percent of manufacturer-recommended full engine speed. Maximum and minimum energy input levels were determined by running full load performance determinations using JP-4 fuel and no load performance determinations using the reference fuel. Maximum fuel flows (at full rack) were reduced slightly to compensate for density and net heat of combustion differences between fuels. Maximum and minimum energy inputs at a given speed were then calculated from these fuel flows. This process produced energy input levels that could be obtained using all the test fuels. Four energy points were placed to span the difference between minimum and maximum energy levels. These four energy levels and three speeds yielded twelve points per test. Table 7 shows a typical run sheet generated by the computer program. In practice, operators could not control fuel flow to the engine with the precision desired.

TABLE 7. TYPICAL RUN SHEET

ENGINE: 4-53T FUEL: AL-10697-F TEST NO: 1

	SPEED (RPM)	FUEL FLOW (LB/HR)
1	2500	53.0
2	2500	44.8
3	2500	36.7
4	2500	28.5
5	1875	44.1
6	1875	35.1
7	1875	26.0
8	1875	17.0
9	1250	19.1
10	1250	15.9
11	1250	12.6
12	1250	9.3

As a result, actual energy points were scattered in the vicinity of the desired energy points. At test completion, it was discovered that net heat of combusion values obtained from the laboratory were also not as accurate as desired. Repeating the net heat of combustion tests several times yielded average values that were more representative of actual values. The correct net heat of combustions were incorporated into the statistical analysis of results. To have an immediate check on the data and to minimize errors, each test was run twice. This duplicate data provided the opportunity to discover and correct many errors immediately rather than waiting for the data analysis phase. The data recording form for each test is shown in Table 8. Table 9 lists the test number, engine, and fuel for each of the tests performed. Tests are actually in groups of two, with the odd-numbered tests preceding the even-numbered replicate tests.

B. Engine Operation

As mentioned previously, some engine operating parameters were controlled to emphasize fuel property differences. Table 10 summarizes the engine operating conditions. Oil temperature was controlled by routing an external source of cooling water through the normal engine-mounted oil cooler. Oil temperature was measured at the oil cooler outlet. Set point for oil temperature was 93°C (200°F). Fuel temperature was controlled by a heat exchanger on the engine fuel inlet line. An external source of cooling water was utilized to bring the fuel to the desired 35°C (95°F) set point. Coolant-out temperature was measured at the thermostat housing of each engine. Coolant temperature control was accomplished by blocking the thermostat in the open position and utilizing an external heat exchanger. The desired coolant-out temperature was 82°C (180°F). Inlet air temperature and humidity were not controlled. Inlet air temperature was measured in the air filter housing of each engine. All data outlined in Table 8 were recorded and entered into an in-house computer data base.

During the course of the test, routine dynamometer load cell checks showed that the load cell used on the 4-53T and LDT-465-1C tests was drifting. Rather than re-calibrating the load cell and invalidating all previous

TABLE 8. DATA RECORDING SHEET

MILITARY ENGINES FUEL REQUIREMENTS
LOG SHEET

ENGINE:_____ FUEL:_____ TEST NO:_____ DATE:_____ PAGE:_____

Technician	10 1	11 2	12 3	4	5	6	7	8	9
Time of day									
Actual speed, RPM									
Load, lb.-ft.									
Fuel consumption, lb./hr. (Flowtron)									
Fuel consumption, lb./hr. (Weighed)									
TEMPERATURES, ° F									
Exhaust before turbo									
Exhaust after turbo									
1 Water inlet									
2 Water outlet									
3 Oil sump									
4 Fuel inlet									
5 Inlet air									
6 Air after compressor									
Air after blower (4-53 only)									
Wet/dry bulb									
7 Oil after cooler									
PRESSURES									
Oil, psig									
Fuel, psig									
Air after blower (4-53 only), psig									
Air after compressor, psig									
Exhaust after turbo, in. Hg									
Air before compressor, in. H_2O									
Barometric, in. Hg									

TABLE 9. LIST OF TESTS RUN

TEST NUMBER	ENGINE	FUEL
1	4-53T	AL-10697-F
2	4-53T	AL-10697-F
3	4-53T	AL-10583-F
4	4-53T	AL-10583-F
5	4-53T	AL-10582-F
6	4-53T	AL-10582-F
7	LDT-465	AL-10697-F
8	LDT-465	AL-10697-F
9	LDT-465	AL-10583-F
10	LDT-465	AL-10583-F
11	LDT-465	AL-10582-F
12	LDT-465	AL-10582-F
13	NTC-350	AL-10697-F
14	NTC-350	AL-10697-F
15	NTC-350	AL-10583-F
16	NTC-350	AL-10583-F
17	NTC-350	AL-10582-F
18	NTC-350	AL-10582-F
19	LDT-465	AL-10811-F
20	LDT-465	AL-10811-F
21	NTC-350	AL-10811-F
22	NTC-350	AL-10811-F
23	4-53T	AL-10811-F
24	4-53T	AL-10811-F
25	3208T	AL-10811-F
26	3208T	AL-10811-F
27	4-53T	AL-10813-F
28	4-53T	AL-10813-F
29	3208T	AL-10813-F
30	3208T	AL-10813-F
31	LDT-465	AL-10813-F
32	LDT-465	AL-10813-F
33	NTC-350	AL-10813-F
34	NTC-350	AL-10813-F
35	3208T	AL-10697-F
36	3208T	AL-10697-F
37	3208T	AL-10582-F
38	3208T	AL-10582-F
39	3208T	AL-10583-F
40	3208T	AL-10583-F
41	3208T	AL-10816-F
42	3208T	AL-10816-F
43	3208T	AL-10807-F
44	3208T	AL-10807-F
45	LDT-465	AL-10816-F
46	LDT-465	AL-10816-F
47	LDT-465	AL-10807-F
48	LDT-465	AL-10807-F
49	NTC-350	AL-10816-F
50	NTC-350	AL-10816-F
51	NTC-350	AL-10807-F
52	NTC-350	AL-10807-F
53	4-53T	AL-10816-F

TABLE 9. LIST OF TESTS RUN (CONT'D)

TEST NO.	ENGINE	FUEL
54	4-53T	AL-10816-F
55	4-53T	AL-10807-F
56	4-53T	AL-10807-F
57	4-53T	AL-10812-F
58	4-53T	AL-10812-F
59	NTC-350	AL-10812-F
60	NTC-350	AL-10812-F
61	LDT-465	AL-10812-F
62	LDT-465	AL-10812-F
63	3208T	AL-10812-F
64	3208T	AL-10812-F
65	4-53T	AL-10804-F
66	4-53T	AL-10804-F
67	NTC-350	AL-10804-F
68	NTC-350	AL-10804-F
69	LDT-465	AL-10804-F
70	LDT-465	AL-10804-F
71	3208T	AL-10804-F
72	3208T	AL-10804-F
73	4-53T	AL-10805-F
74	4-53T	AL-10805-F
75	NTC-350	AL-10805-F
76	NTC-350	AL-10805-F
77	LDT-465	AL-10805-F
78	LDT-465	AL-10805-F
79	3208T	AL-10805-F
80	3208T	AL-10805-F
81	4-53T	AL-10806-F
82	4-53T	AL-10806-F
83	NTC-350	AL-10806-F
84	NTC-350	AL-10806-F
85	LDT-465	AL-10806-F
86	LDT-465	AL-10806-F
87	3208T	AL-10806-F
88	3208T	AL-10806-F
89	4-53T	AL-10808-F
90	4-53T	AL-10808-F
91	NTC-350	AL-10808-F
92	NTC-350	AL-10808-F
93	LDT-465	AL-10808-F
94	LDT-465	AL-10808-F
95	3208T	AL-10808-F
96	3208T	AL-10808-F
97	4-53T	AL-10809-F
98	4-53T	AL-10809-F
99	NTC-350	AL-10809-F
100	NTC-350	AL-10809-F
101	LDT-465	AL-10809-F
102	LDT-465	AL-10809-F
103	3208T	AL-10809-F
104	3208T	AL-10809-F
105	4-53T	AL-10810-F
106	4-53T	AL-10810-F
107	NTC-350	AL-10810-F
108	NTC-350	AL-10810-F
109	LDT-465	AL-10810-F
110	LDT-465	AL-10810-F
111	3208T	AL-10810-F
112	3208T	AL-10810-F
113	4-53T	AL-10814-F

TABLE 9. LIST OF TESTS RUN (CONT'D)

TEST NO.	ENGINE	FUEL
114	4-53T	AL-10814-F
115	NTC-350	AL-10814-F
116	NTC-350	AL-10814-F
117	LDT-465	AL-10814-F
118	LDT-465	AL-10814-F
119	3208T	AL-10814-F
120	3208T	AL-10814-F
121	4-53T	AL-10815-F
122	4-53T	AL-10815-F
123	NTC-350	AL-10815-F
124	NTC-350	AL-10815-F
125	LDT-465	AL-10815-F
126	LDT-465	AL-10815-F
127	3208T	AL-10815-F
128	3208T	AL-10815-F
129	4-53T	AL-10817-F
130	4-53T	AL-10817-F
131	NTC-350	AL-10817-F
132	NTC-350	AL-10817-F
133	LDT-465	AL-10817-F
134	LDT-465	AL-10817-F
135	3208T	AL-10817-F
136	3208T	AL-10817-F
137	4-53T	AL-10818-F
138	4-53T	AL-10818-F
139	NTC-350	AL-10818-F
140	NTC-350	AL-10818-F
141	LDT-465	AL-10818-F
142	LDT-465	AL-10818-F
143	3208T	AL-10818-F
144	3208T	AL-10818-F
145	4-53T	AL-10999-F
146	4-53T	AL-10999-F
147	NTC-350	AL-10999-F
148	NTC-350	AL-10999-F
149	LDT-465	AL-10999-F
150	LDT-465	AL-10999-F
151	3208T	AL-10999-F
152	3208T	AL-10999-F
153	4-53T	AL-11017-F
154	4-53T	AL-11017-F
155	NTC-350	AL-11017-F
156	NTC-350	AL-11017-F
157	LDT-465	AL-11017-F
158	LDT-465	AL-11017-F
159	3208T	AL-11017-F
160	3208T	AL-11017-F

TABLE 10. SUMMARY OF OPERATING CONDITIONS

Engine Oil	4-53T AL-7074-L	LDT-465-1C AL-7074-L	NTC-350 AL-7074-L	3208-T AL-7074-L
Oil Temperature, °C(°F)				
Minimum	92 (198)	92 (198)	90 (194)	81 (178)
Maximum	97 (207)	98 (209)	98 (209)	98 (209)
Average	94 (202)	94 (201)	93 (200)	93 (200)
Fuel Temperature, °C(°F)				
Minimum	34 (94)	31 (87)	32 (89)	29 (85)
Maximum	36 (97)	36 (97)	37 (99)	37 (98)
Average	35 (95)	35 (95)	34 (93)	34 (93)
Coolant-Out Temperature, °C (°F)				
Minimum	81 (177)	80 (176)	79 (175)	80 (176)
Maximum	84 (183)	86 (186)	84 (183)	83 (182)
Average	82 (180)	82 (180)	82 (180)	82 (179)
Inlet Air Temperature, °C (°F)				
Minimum	31 (87)	24 (75)	26 (78)	26 (79)
Maximum	42 (108)	43 (110)	38 (100)	43 (110)
Average	36 (97)	37 (98)	32 (89)	34 (93)
Speeds, RPM				
100%	2500	2600	2100	2800
75%	1875	1950	1575	2100
50%	1250	1300	1050	1400
Load, N•M (lb-ft)				
Minimum	90 (66.4)	56.7 (41.8)	50 (36.9)	23.7 (17.5)
Maximum	435.9 (321.5)	525 (387.2)	1155.3 (852.0)	544 (401.2)
Energy Input, Btu/injection				
Minimum	0.555	0.731	0.908	0.476
Maximum	1.863	3.332	6.246	2.007
Maximum Power Output During Test, kW (BHP)	102 (136.4)	107 (143.5)	202 (270.7)	99 (132.6)

tests, periodic checks were made of the drift. At the conclusion of the test, the drift was plotted against time and found to be roughly linear. A correction factor was then introduced to correct the affected loads based on the test date. This was implemented through the computer system.

During statistical analysis of the fuel properties, the computer program BMDP1R revealed high correlations between many fuel properties. Underlined values in Appendix B indicate high correlations between properties. It was deemed inadvisable to include highly correlated properties in further analysis due to the duplicate information contained in the properties. Therefore, since 50-percent boiling point was highly correlated with viscosity, 50-percent boiling point was dropped from further analysis. Next, BMDP1R was used to develop linear regression equations for the four engines. Initially, load was the dependent variable, and speed, speed squared, energy, energy squared, and speed times energy were the independent variables. Speed squared and energy squared correlated well with speed and energy, respectively, so they were dropped from further analysis. Next, the fuel properties viscosity, aromatic content, 10-percent boiling point (10%BP), and cetane number were introduced into the analysis. Multiple linear regression analysis of the data using the computer program BMDP1R yielded load equations for the engines.

The equation for the Detroit Diesel 4-53T with speeds of 1250-2500 rpm (50-100% of full speed) is:

Load = 5.43158 - 0.02564 Speed + 166.9574 Energy + 0.01699 Speed Energy - 0.15976 Aromatic Content - 0.0001 10%BP + 0.13093 Viscosity - 0.08676 Cetane Number

The equation for the Continental Motors LDT-465-1C with speeds of 1300-2600 rpm (50-100% of full speed) is:

Load = 29.25141 - 0.04308 Speed + 114.98773 Energy + 0.01298 Speed Energy - 0.11661 Aromatic Content - 0.02770 10%BP - 0.08003 Viscosity - 0.14092 Cetane Number

The equation for the Caterpillar 3208T with speeds of 1400-2800 rpm (50-100% of full speed) is:

Load = 2.77937 - 0.04426 Speed + 235.20103 Energy + 0.00146 Speed Energy - 0.11902 Aromatic Content - 0.00074 10%BP + 1.59395 Viscosity - 0.09825 Cetane Number

The equation for the Cummins NTC-350 with speeds of 1050-2100 rpm (50-100% of full speed) is:

Load = 109.86153 - 0.1151 Speed + 116.04908 Energy + 0.02703 Speed Energy - 0.17976 Aromatic Content - 0.00387 10%BP + 0.582 Viscosity - 0.12697 Cetane Number

Units for these equations are: Load - lb-ft, Speed - rpm, Energy - Btu/injection, Aromatic Content - vol% by FIA, 10%BP - °F by ASTM Method D 86, Viscosity at 40°C - cSt, and Cetane Number - no units.

Tables 11 through 14 summarize the statistics associated with each of these equations. An attempt was made to correlate residuals (residual=predicted value-observed value for each point) with fuel properties, but no strong correlations were found. Several methods were tried in order to rank each test fuel in relation to the reference fuel. Average loads produced by each fuel were compared under the premise that each fuel was subjected to exactly the same energy input levels. In reality, however, human and experimental error scattered the energy points slightly. While this did not adversely affect the load equations, it did invalidate ranking schemes.

C. Cross Validations

Two additional fuels were run through the test program after load equations had been obtained for the eighteen test fuels. These fuels had been blended for a separate program but were included herein to obtain some cross validations. Predicted loads obtained from the equations on the preceding page are compared with observed loads in Figures 6 through 9.

TABLE 11. MULTIPLE LINEAR REGRESSION STATISTICS FOR THE 4-53T ENGINE

Engine: 4-53T
Data Points: 432 (18 fuels x 24 data points per fuel)
Multiple R-Square: 0.9919
Standard Error of Estimate: 6.5175

Variable	Coefficient	Std. Error	T
Intercept	5.43158		
Speed	-0.02564	0.002	-10.484*
Energy	166.95740	4.264	39.156*
Speed x Energy	0.01699	0.002	7.707*
Aromatics	-0.15976	0.068	-2.357*
10% BP	-0.00010	0.006	-0.017
Viscosity	0.13093	1.220	0.107
Cetane	-0.08676	0.157	-0.552

*Significant quantity ($|T| > 2$). T is a standard statistical method for expressing the significance of a coefficient. T is equal to the estimated coefficient divided by the standard deviation for that coefficient.

TABLE 12. MULTIPLE LINEAR REGRESSION STATISTICS FOR THE LDT-465-1C ENGINE

Engine: LDT-465-1C
Data Points: 432 (18 fuels x 24 data points per fuel)
Multiple R-Square: 0.9810
Standard Error of Estimate: 13.989

Variable	Coefficient	Std. Error	T
Intercept	29.25141		
Speed	-0.04308	0.004	-10.524*
Energy	114.98773	3.550	32.388*
Speed x Energy	0.01298	0.002	6.412*
Aromatics	-0.11661	0.145	-0.802
10% BP	-0.02770	0.013	2.153*
Viscosity	-0.08003	2.619	-0.031
Cetane	-0.14092	0.338	-0.417

*Significant quantity ($|T| > 2$)

TABLE 13. MULTIPLE LINEAR REGRESSION STATISTICS FOR THE NTC-350 ENGINE

Engine: NTC-350
Data Points: 432 (18 fuels x 24 data points per fuel)
Multiple R-Square: 0.9946
Standard Error of Estimate: 19.438

Variable	Coefficient	Std. Error	T
Intercept	109.86153		
Speed	-0.11510	0.005	-22.527*
Energy	116.04908	2.156	53.814*
Speed x Energy	0.02703	0.001	18.229*
Aromatics	-0.17976	0.202	-0.889
10% BP	-0.00387	0.018	-0.217
Viscosity	-0.58200	3.639	0.160
Cetane	-0.12697	0.469	-0.271

*Significant quantity (|T| >2)

TABLE 14. MULTIPLE LINEAR REGRESSION STATISTICS FOR THE 3208T ENGINE

Engine: 3208T
Data Points: 432 (18 fuels x 24 data points per fuel)
Multiple R-Square: 0.9944
Standard Error of Estimate: 8.3879

Variable	Coefficient	Std. Error	T
Intercept	2.77937	0.002	
Speed	-0.044426	3.241	-21.553*
Energy	235.20103	0.087	72.561*
Speed x Energy	-0.00146	0.002	-0.900
Aromatics	-0.11902	0.087	-1.365
10% BP	-0.00074	0.008	-0.096
Viscosity	1.59395	1.570	1.015
Cetane	-0.09825	0.202	-0.485

*Significant quantity (|T| >2)

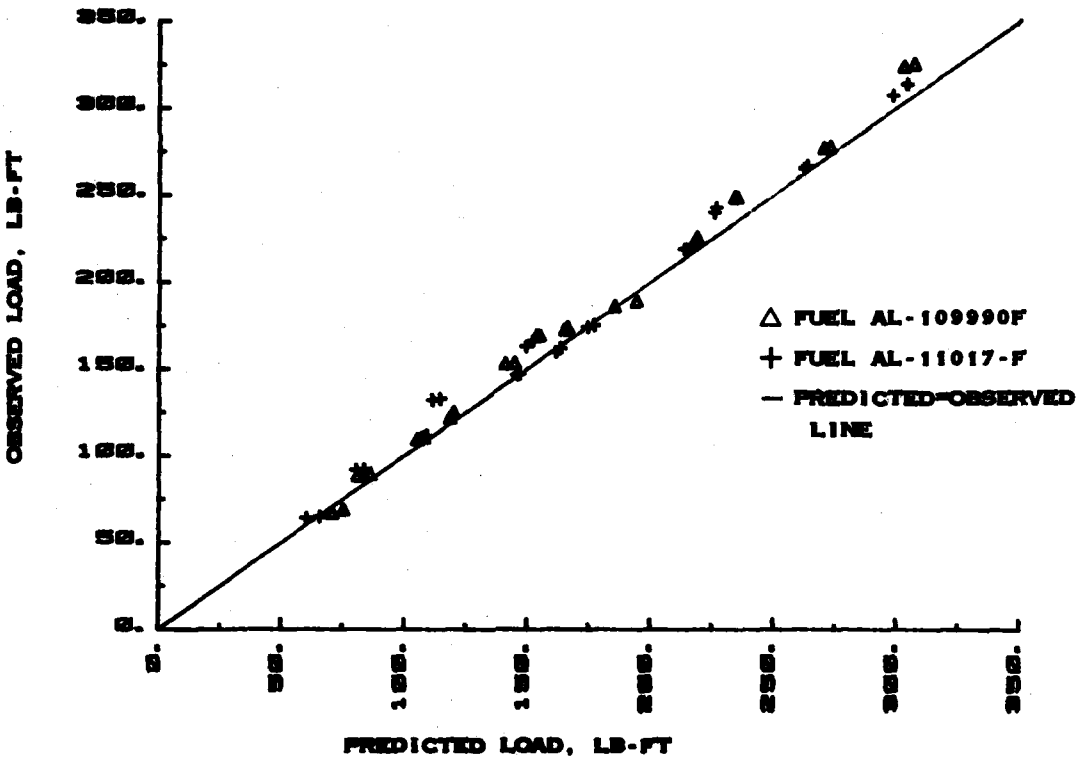

FIGURE 6. PREDICTED VS OBSERVED LOAD IN THE 4-53T ENGINE

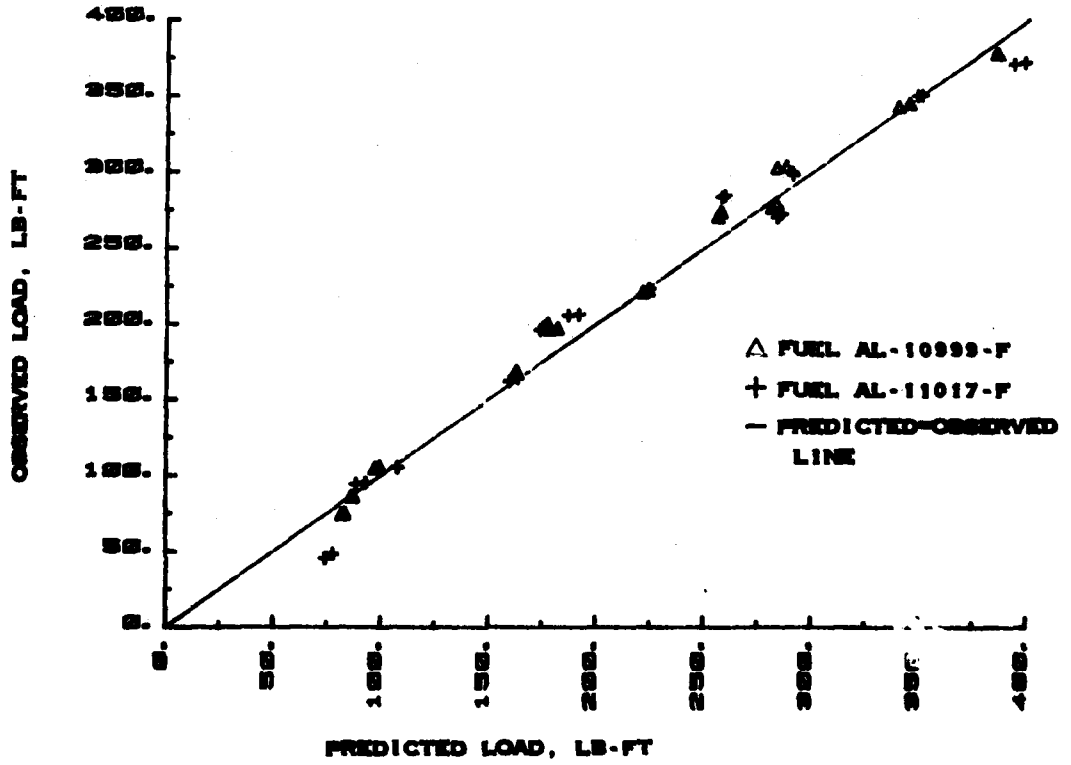

FIGURE 7. PREDICTED VS OBSERVED LOAD IN THE LDT-465-1C ENGINE

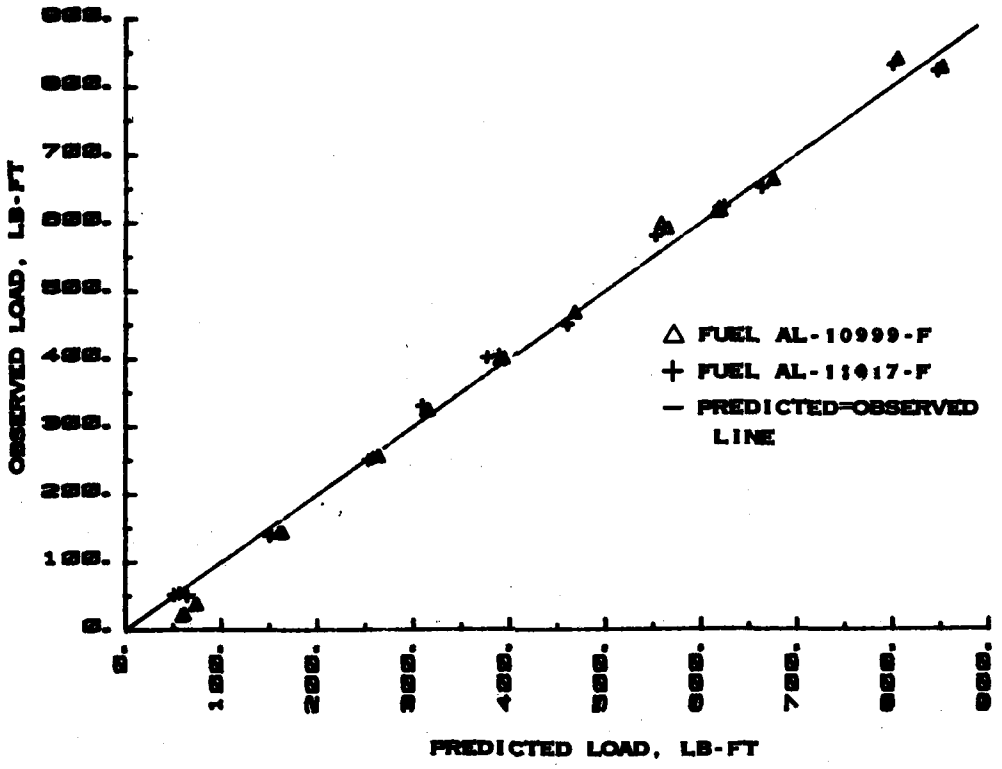

FIGURE 8. PREDICTED VS OBSERVED LOAD IN THE NTC-350 ENGINE

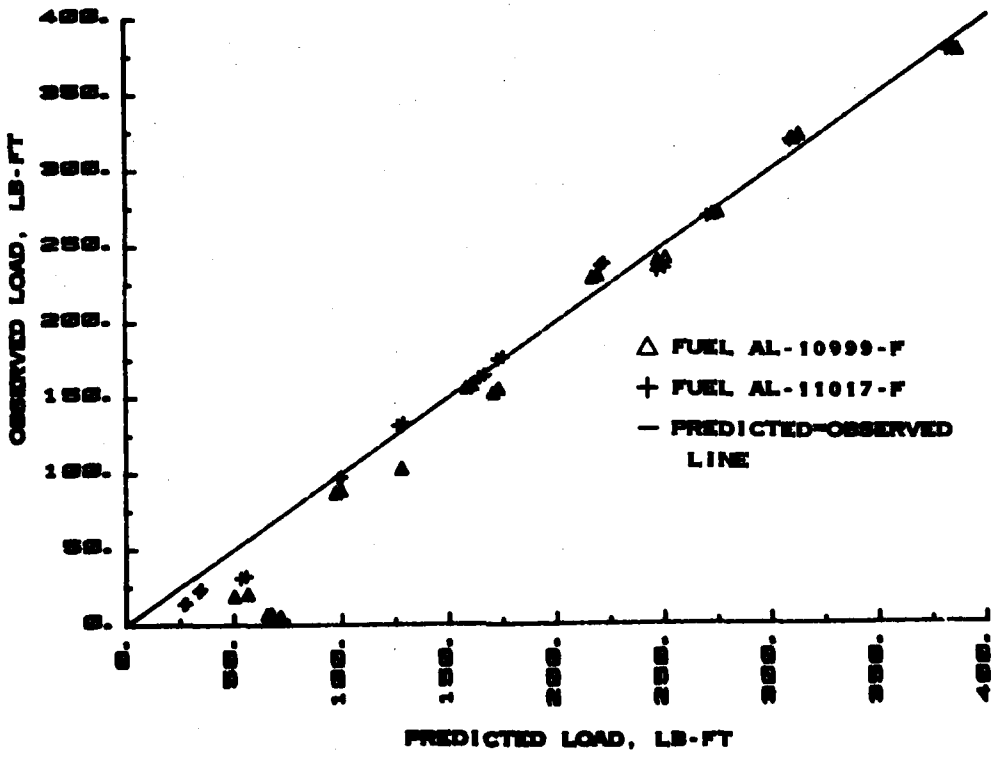

FIGURE 9. PREDICTED VS OBSERVED LOAD IN THE 3208T ENGINE

Figure 6 shows the results for the 4-53T engine and indicates that the prediction equation was slightly low in its prediction for both fuels. A least squares curve fit on the observed vs. predicted data yields the equation $Y = 3.8889 + 1.0118X$, with an R^2 value of 0.99054. Ideally this equation would be $X = 0 + 1.0X$. This ideal observed = predicted line is shown in Figures 6 through 9.

Figure 7 shows the results using the LDT-465-1C engine. The prediction equation seems to have fit the data quite well except at the low load low speed points using fuel 20 (AL-11017-F). A least squares curve fit on the predicted vs. observed data yields the equation $Y = -29.082 + 1.058X$ with an R^2 value of 0.99361.

Results for the NTC-350 engine are shown in Figure 8. A least squares curve fit yields the equation of $Y = 6.6832 + 0.9823X$ with an R^2 value of 0.97940.

The cross-correlation points for the 3208T engine are shown in Figure 9. Observed values were lower than the predicted values, particularly at the low load low speed points. This probably indicates that load has nonlinear tendencies at low speed/load combinations when this engine-fuel combination is used. This trend is not evident in the 18-fuel analysis presented earlier. A least squares curve fit yields the equation $Y = -5.6282 + 1.0167X$ with an R^2 value of 0.99656.

D. Discussion of Results

The results presented herein represent the testing of eighteen fuels in four different engines under controlled laboratory conditions. The equations and results discussed should not be construed as universally applicable to each engine. This would require testing many engines of a particular model in order to account for engine-to-engine variability. Every attempt has been made to preserve accuracy, and results may be interpreted as representative of a particular engine's operations under the given conditions. All tests were short term and do not address long-term durability problems, such as

pump wear or carbon buildup which may result from the use of non-specification fuels.

None of the engines was run at manufacturer's rated full power. This fact was due to the test matrix requirement that fuels be tested at the same energy levels. Maximum fuel flow to an engine is generally controlled volumetrically by the fuel injection system. Low-viscosity fuels generally produce higher internal leakage than high-viscosity fuels. At full rack, an engine will generally consume more (volumetrically) of a high-viscosity fuel than a low-viscosity fuel. To attain the same energy levels (Btu/injection) for all fuels, it was necessary to choose maximum and minimum energy points that could be attained by all fuels. Because of viscosity and net heat of combustion differences between fuels, all engines were run at maximum powers lower than that attainable with No. 2 diesel fuel (see Table 10 for maximum powers during test and Figures 2 through 5 for rated powers). This is particularly significant for the Caterpillar 3208T engine which was previously derated by a factory error in fuel system setup. Thus, all results on the 3208T engine should be viewed in light of the fact that the engine was operated well below its maximum power curve and probably low on its brake specific energy consumption curve. This is also true of the other engines, but to a lesser extent.

The multiple linear regression analyses presented in Tables 11 through 14 indicate many things about the combustion processes taking place in these engines. The dominant variable in all four analyses is, of course, energy input. The energy coefficients, when divided by the number of injections per revolution, allow a look at the efficiencies of the four engines. This number reveals that, for a given energy input (fuel flow), engines with larger coefficients produce greater load. In this study, the Caterpillar 3208T is the most efficient, followed by the DD 4-53T engine. The Cummins NTC-350 and the Continental Motors LDT-465-1C tie for third place.

In all four analyses, speed has a negative and significant impact on load. This is to be expected, since engine friction increases with speed. By controlling oil temperature at 93°C (200°F), much of the viscosity change

associated with higher speeds and loads was eliminated. The speed coefficient, therefore, represents combustion losses and friction losses. It is not possible to compare speed coefficients of different engines due to the varying speeds and oil pressures.

The speed times energy coefficient represents the interaction of speed and energy. In the three cases where the term is significant, it has a positive value. This seems to indicate that high speed-energy conditions yield higher loads in three of the four engines. The 3208T engine did not yield a significant coefficient for speed times energy; therefore, little can be said about it.

The DD 4-53T engine seems to be sensitive to the aromatic content of the fuel. This is indicated by the significant negative coefficient that this variable displays. For a rise in aromatic content, a drop in load can be expected. While this effect is small, it does appear to be significant ($|T| = 2.357$).

The 4-53T engine did not appear to be significantly affected by changes in 10%BP, viscosity, or cetane number. Load was expected to be adversely affected by low cetane numbers, but the regression analysis did not indicate this. Although the coefficient for cetane number is not statistically significant (we have less confidence in its validity), it is slightly negative. This negative factor seems to indicate that the ignition delay produced by a low cetane fuel is beneficial to the combustion process in this engine. This would be true only to a certain point. Since the test fuels spanned the cetane numbers from 31.3 to 53.1, it may be that the range did not dip low enough to adversely affect performance. Low-temperature startability would also be affected by low cetane numbers. No cold starts were performed in this test series, due to warm weather and lack of equipment.

The Continental Motors LDT-465-1C seemed to be sensitive to the 10%BP of the fuel. The coefficient indicates that as TPBP increases, load decreases slightly. The LDT-465-1C engine employs a MAN combustion system in which the rate of combustion is controlled by the rate of vaporization of the fuel. High 10%BP fuels should vaporize more slowly than low TPBP fuels.

The LDT-465-1C engine does not seem to be cetane-sensitive in the range of cetane numbers explored. This was expected, due to the multi-fuel design of this engine and its historical cetane tolerance. The engine did not appear to be sensitive to either viscosity or aromatic content over the ranges tested. The MAN combustion system was expected to be viscosity-tolerant since combustion depends on vaporization rather than atomization.

The Cummins NTC-350 engine did not appear to be sensitive to either aromatic content, 10%BP, viscosity, or cetane number. Indeed, none of the coefficients for these variables was statistically significant. This indicates that over the range of properties tested, this engine is quite fuel-tolerant in terms of performance.

The Caterpillar 3208T engine was not significantly affected by aromatic content, 10%BP, viscosity, or cetane number. Although the coefficients of these variables were not statistically significant, aromatic content and viscosity seemed to have had a small effect. Higher aromatic contents may produce slightly lower loads, while higher viscosities may produce slightly higher loads. This engine seems to be quite fuel-tolerant over the range of properties tested. The 3208T engine was run well below its maximum power, due to improper fuel system setup.

IV. GAS TURBINE EXPERIMENTAL PROGRAM

Combustion performance measurements on twenty test fuels were performed in a T-63 combustor at realistic operating conditions. The first eighteen test fuels were for the "Military Engine Fuel Requirements" program, and fuels 19 and 20 were included as part of the "Multifuels Engine Development" program. A low aromatic Jet A (fuel 0) was used as a reference fuel in the measurements. The areas investigated for fuel sensitivity were:

- Ignition
- Flame Radiation

- Exhaust smoke
- Gaseous emissions (THC, CO, and NO_x)
- Combustion efficiency

A. Combustor Facilities

This work was performed in the U.S. Army Fuels and Lubricants Research Laboratory (AFLRL), located at Southwest Research Institute, with the Army's permission. This facility was specially designed to study fuel-related problems in the operation of turbine engines. The air supply system provides a clean, smooth flow of air to the combustion test cell at rates up to 1.1 kg/s at pressures to 1620 kPa (16 atm) and temperatures to 1100K (unvitiated). Turbine flow meters and strain-gage pressure transducers are used to measure flow properties of the air and fuel. Thermocouples are referenced to a 339K (150°F) oven. Data reduction is performed on-line with test summaries available immediately; these summaries provide average flow data as well as standard deviations (typically less than 1 percent of average values), exhaust temperature profiles, and emissions data and combustion efficiency.

B. Combustor Rig

The combustor rig is based on engine hardware from the Allison T-63 engine. (5, 6) The burner shown in Figure 10 is a single-can type with a dual-orifice pressure atomizer centered in the dome. At the burner exit, there is a centerbody that directs the flow into an annulus where the nozzles and turbine blades are normally located. Gas-sampling probes, pressure probes, and thermocouples are arranged circumferentially in one plane of this annulus at various radial positions. Table 15 presents the air flow and fuel flow conditions that were established to correspond with various power points following the guidelines of the manufacturer.

Exhaust smoke was measured in accordance with SAE-ARP1179, and flame radiation from the primary zone was measured with a water-cooled bolometer-type radiation sensor attached to the side of the liner. The sensor had a

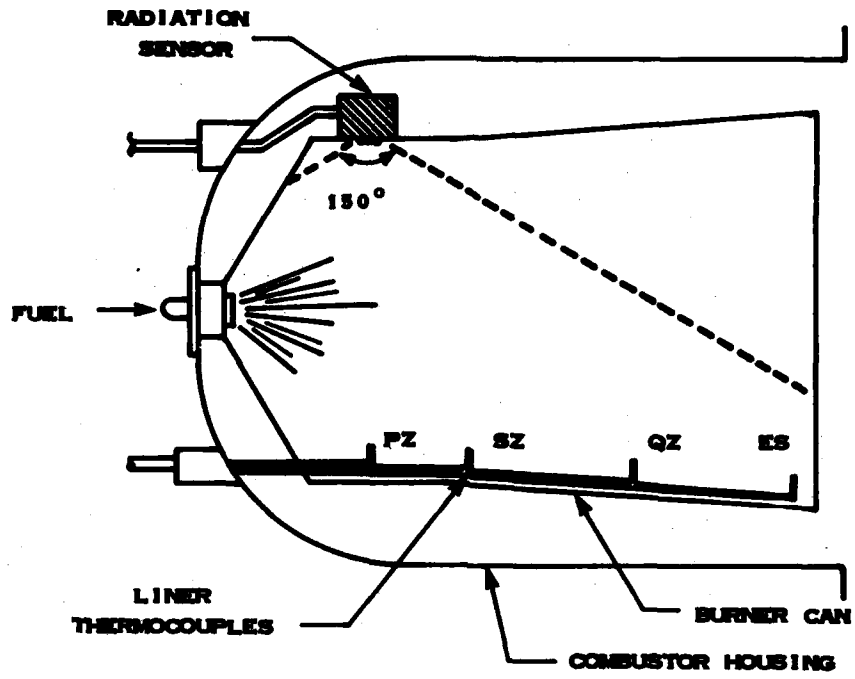

FIGURE 10. T-63 COMBUSTOR

TABLE 15. T-63 COMBUSTOR RIG OPERATING CONDITIONS

Mode	% Full Power	BIP, psia	BIT, °F	Wa, lb/s	Wf, lb/m	F/A
Ground Idle	10	33.4	300	1.40	0.92	0.0109
Cruise	55	53.6	430	2.06	1.79	0.0145
Climb	75	60.7	472	2.24	2.23	0.0166
Takeoff	100	69.2	524	2.42	2.87	0.0198

sapphire window and a viewing angle of 150 degrees. Gaseous emissions (CO, CO_2, NO, NO_2, O_2, and THC) were also measured, and combustion efficiency was calculated from the exhaust gas analysis. The NO and NO_2 measurements were combined and reported as NO_x.

C. Experimental Results and Discussion

For gas turbine combustors, the fuel properties of greatest concern are the composition, the distillation curve, and the viscosity. The first property is generally associated with flame radiation and exhaust smoke; the latter two affect atomization and vaporization, and therefore, ignition, gaseous emissions, and combustion efficiency. The measurements of the flame radiation, exhaust smoke, gaseous emissions and combustion efficiency for the test fuels 0-20 are given in tabular form in Appendix B.

D. Radiation and Smoke

Soot formed in gas turbine engines is observed in the form of exhaust smoke and increased combustion chamber liner temperatures, i.e., radiant heat transfer from incandescent carbon particles (10). The flame radiation intensity is a function of the gas temperature and the flame emissivity which depends on soot concentration. Exhaust smoke is what remains after about 98 percent (11) of the soot is oxidized in the secondary and quench zones of the combustor; these oxidation rates are dependent on combustor operating conditions such as burner inlet temperature, and not on fuel properties. Therefore, exhaust smoke number measurements are normally consistent with flame radiation studies.

Several studies (5-7, 12-13) have shown that hydrogen content (H/C ratio) correlates more consistently with the sooting tendency of fuels than the traditional properties, smoke point, and aromatic content. The effects of end point and viscosity are not important because soot is formed in the gas phase and not by the pyrolysis of fuel droplets. However, carbon formed solely by gas phase reactions at conditions of high-combustion efficiency should be distinguished for carbon deposits formed at low-combustion effi-

ciency conditions by the pyrolysis of fuel droplets on the combustion chamber walls. This aspect of carbon formation was not addressed in the present study.

The correlation of the sooting tendency with H/C ratio is generally assumed to be a linear function of the H/C ratio. However, when the sooting tendency is measured over a wide range of H/C ratios, there is evidence for significant curvature in the correlation. Earlier studies on the effects of fuel properties on flame radiation and exhaust smoke in the T-63 combustor for the U.S. Navy (5) and the U.S. Air Force (14) have produced a data bank which includes fuels with H/C ratios ranging from about 1.5 to 2.5. These test fuels varied significantly in composition, including petroleum base, syncrudes, water-in-fuel macroemulsions, microemulsions of water-in-fuel, and alcohol-fuel solutions. Flame radiation intensity measurements on the fuels taken at the full power operating condition of the T-63 burner were found to correlate favorably with H/C ratio. However, the plot of radiation (R) versus H/C ratio was not a straight line; instead, it appeared as an exponential dependence of R on H/C ratio. Figure 11 shows that an exponential model gives a surprisingly good correlation (CC = 0.934) of R and H/C ratio. This method of correlating R and H/C ratio is used in the present study because it also correlates well with these data and may have predictive value. Figures 12 and 13 show the respective correlations of flame radiation and exhaust smoke number with H/C ratio. The least squares fit to the data is based on Fuels 0-18. It is apparent that the flame radiation and exhaust smoke from Fuels 0-18 correlate very well with H/C ratio. The slight deviations from the correlations that are apparent can be attributed to scatter in the data because they are not consistent in the correlations of both radiation and smoke. If a fuel shows high flame radiation, it should also give a high smoke number. Fuels 19 and 20 show significant deviations from the correlations of both the flame radiation and the exhaust smoke with H/C ratio. Fuel 20 had a very low H/C ratio which may be outside the limits of the correlation. It is interesting to note that the H/C ratio of virgin soot is near unity. Not until the soot particles have been heated and oxidized by the exhaust gases in the secondary and quench zones of the combustor is most of the hydrogen lost. It stands to reason, then, that the

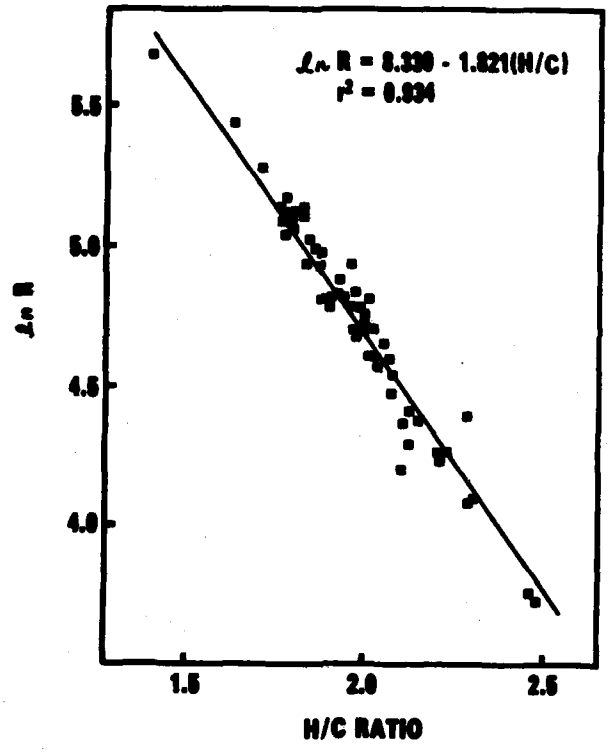

FIGURE 11. CORRELATION OF FLAME RADIATION WITH H/C RATIO IN A T-63 GAS TURBINE COMBUSTOR

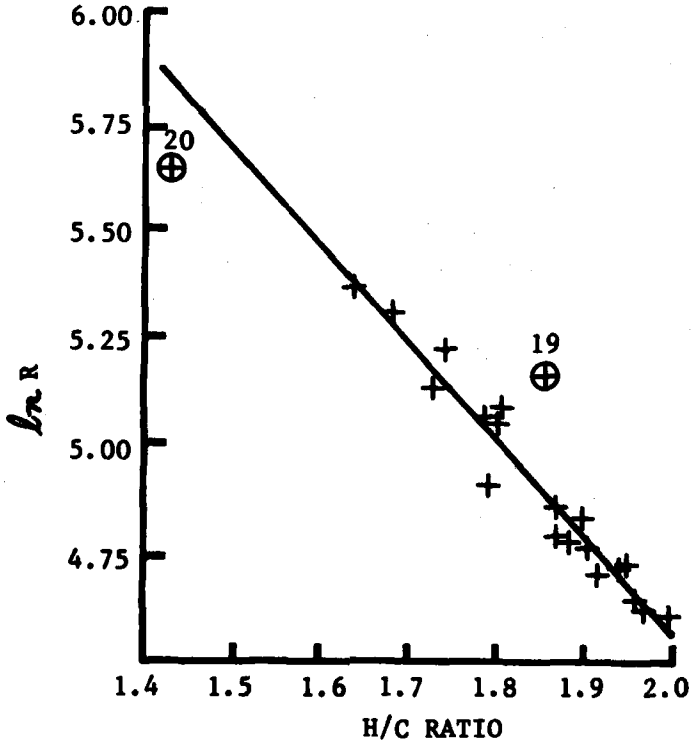

FIGURE 12. CORRELATION OF FLAME RADIATION WITH H/C ATOM RATIO

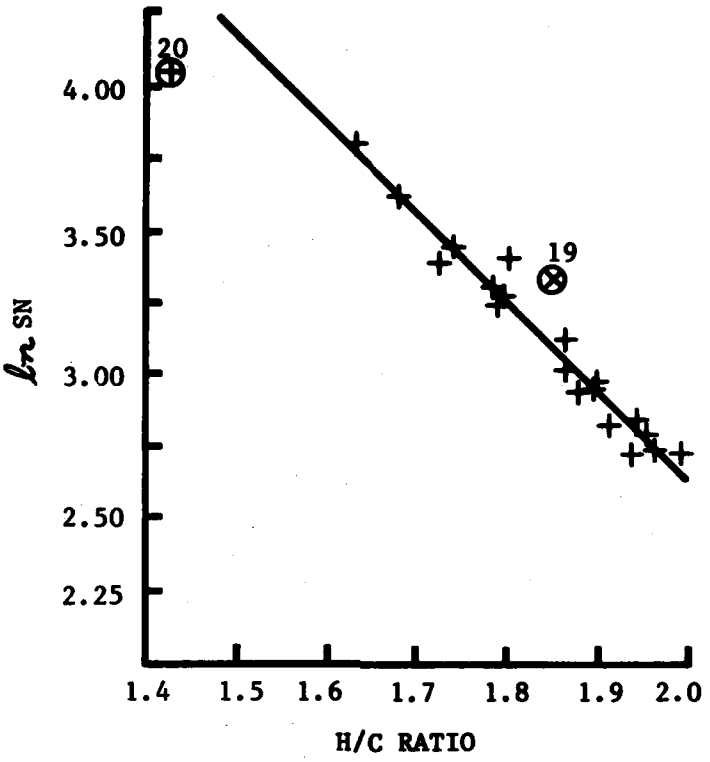

FIGURE 13. CORRELATION OF EXHAUST SMOKE NUMBER WITH H/C ATOM RATIO

correlation of sooting tendency with H/C ratio would break down at H/C ratios near unity. The relatively high values of both radiation and smoke from Fuel 19 are most unusual. Note, Fuels 19 and 20 were tested at a different time than Fuels 0 through 18. It is possible that some change occurred in the flame even though the operating conditions were the same.

E. Gaseous Emissions and Combustion Efficiency

The gaseous emissions (THC, CO, and NO_x) were measured at each of the test conditions: idle, cruise, climb, and takeoff. The THC and CO emissions are predominant at the idle condition where combustion is limited by the rates of fuel vaporization and mixing. At the higher power operating conditions, the emissions of hydrocarbons and CO are relatively low and virtually independent of fuel properties. The fuel properties that affect vaporization are the viscosity and the boiling point distribution. Viscosity affects

fuel atomization and droplet size, while the boiling point distribution determines the rate of droplet vaporization. The end point of the boiling point distribution is expected to correlate with THC emissions because the highest boiling point components of the droplets are least likely to vaporize and burn.

The rate of oxidation of CO is limited by the mixing processes in the burner at low power operating conditions, and is not expected to be greatly dependent on fuel properties. However, the characteristic time allowed for mixing is dependent on the time required for fuel vaporization, so the CO emissions index is indirectly tied to the fuel properties that affect the THC emissions index.

A multiple variable linear regression analysis technique was used in correlating the THC, CO emissions indices, and the combustion efficiency (ε), with the fuel viscosity (V) and end point (EP). A simple polynomial model of the type

$$\text{Emissions Index} = K + a \cdot V + b \cdot V^2 + c \cdot EP + d \cdot EP^2$$

was used. The values of the coefficients are listed in Table 16. Figures 14 and 15 show the results of the correlations, i.e., the observed versus predicted values. It is apparent that the correlation coefficients are quite low (≈ 0.5) since the points scatter widely about the diagonal.

TABLE 16. CORRELATION COEFFICIENTS

Emissions Index	K	a	b	c	d
THC	154.8	-44.3	10.60	0	3.5×10^{-4}
CO	106.5	-0.42	3.45	0.034	0
(100-ε)	3.9	-0.78	0.175	7.9×10^{-3}	0
THC + 12 CO/28	164.8	-47.6	12.65	0.252	0

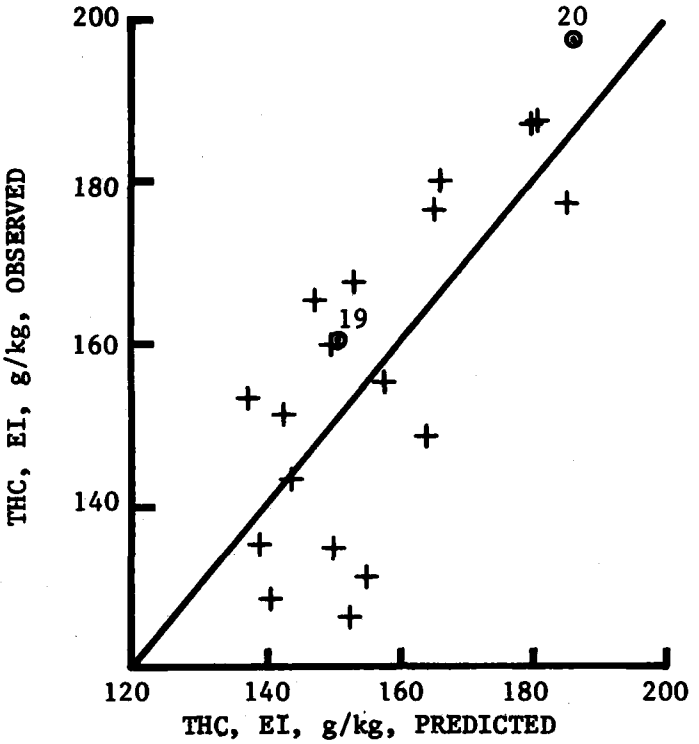

FIGURE 14. CORRELATION OF TOTAL HYDROCARBONS EMISSIONS INDEX WITH FUEL VISCOSITY AND END POINT; OBSERVED VERSUS PREDICTED VALUES

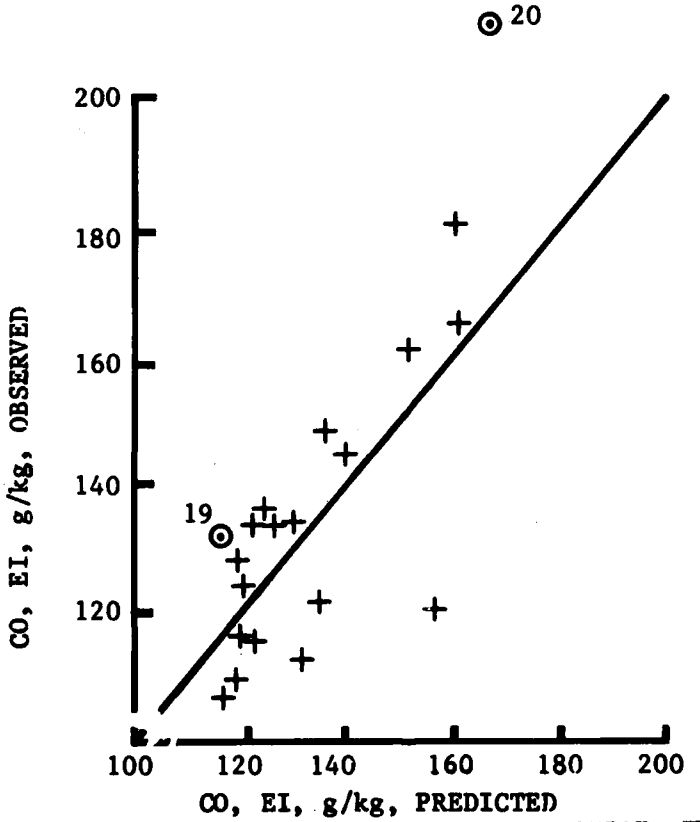

FIGURE 15. CORRELATION OF CARBON MONOXIDE EMISSIONS INDEX WITH FUEL VISCOSITY AND END POINT; OBSERVED VERSUS PREDICTED VALUES

However, the regression analyses gives expected trends and indicates that the THC and CO emissions indices are more strongly dependent on viscosity than end point. This suggests that droplet size is the more important parameter in the fuel vaporization process for Fuels 1 through 18.

The correlations predict reasonable trends in the THC and CO emissions indices of Fuels 19 and 20. Fuel 19 has a low viscosity and end point, and its THC and CO indices are correspondingly on the low side. Fuel 20 has an unusually high viscosity and end point and its emissions indices were higher than any of the other test Fuels 1 through 18.

Combustion efficiencies tabulated in Appendix B were calculated from the exhaust gas analysis according to a relationship developed by Hardin.(15)

$$\varepsilon = \left[1 - \left(\frac{A \cdot f(THC) - 121{,}745 \cdot f(CO) - 38{,}880 \cdot f(NO) - 14{,}644 \cdot f(NO_2)}{A \cdot [f(CO_2) + f(CO) + f(THC)]}\right)\right] \cdot 100$$

where f(i) is the concentration of "i" in the exhaust and A is a constant based on the heat of combustion and H/C ratio of the fuel. This combustion efficiency is a ratio of the energy actually released in the reaction to the energy that would have been realized if the fuel were totally oxidized to CO_2 and H_2O. The combustion inefficiency ($100-\varepsilon$) is determined, for the most part, by the THC and CO emissions, and therefore, should correlate with fuel viscosity and end point at low power operating conditions. Figure 16 shows a plot of the calculated (experimental) versus predicted values of ($100-\varepsilon$) from the multiple linear regression analysis; the constants in the equation are given in Table 16. This correlation based on Fuels 1 through 18 has a very weak correlation coefficient (≈ 0.4), but nevertheless, predicts the basic trends in the relative values of ($100-\varepsilon$) for Fuels 19 and 20. Actually, in the equation given above for calculating the combustion efficiency, it is assumed that the H/C ratio of the THC's is the same as that of the neat fuel. This is probably in error, because some hydrogen may be lost due to partial oxidation of the hydrocarbons that escape. Since THC and CO represent the incompleteness of the oxidation process, it is sug-

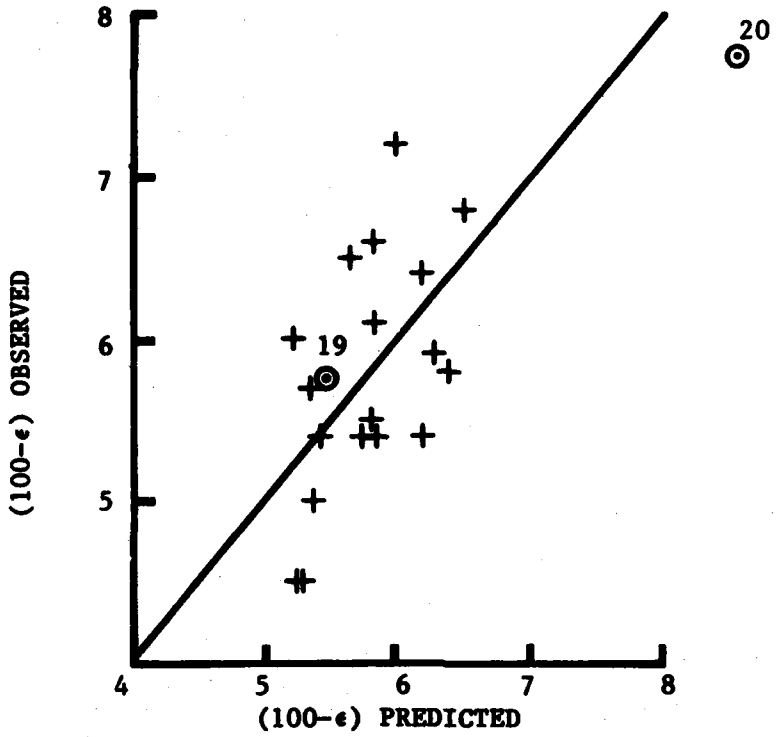

FIGURE 16. CORRELATION OF COMBUSTION INEFFICIENCY WITH FUEL VISCOSITY AND END POINT: OBSERVED VERSUS PREDICTED VALUES

gested that some combination of THC and CO would give a more favorable correlation. The quantity (THC + 12 CO/28) was chosen because it seems to be a better measure of the amounts of carbon and hydrogen that escaped oxidation. The constant 12/28 is simply the ratio of the atomic weight of carbon to the molecular weight of CO. Figure 17 shows the observed versus predicted values of (THC + 12 CO/28) based on the equation and the constants in Table 16 obtained from the multiple linear regression technique. The results indicate that the quantity (THC + 12 CO/28) correlates more favorably (C.C. = 0.65) with viscosity and end point than either of the individual quantities THC, CO, or (100-ε). This correlation predicts the trends in Fuels 19 and 20 with about the same accuracy as the other correlations.

F. NOx Emissions

Oxides of nitrogen (NO_x) can form by the oxidation of molecular nitrogen in the air or chemically bound nitrogen in the fuel. The oxidation of molecu-

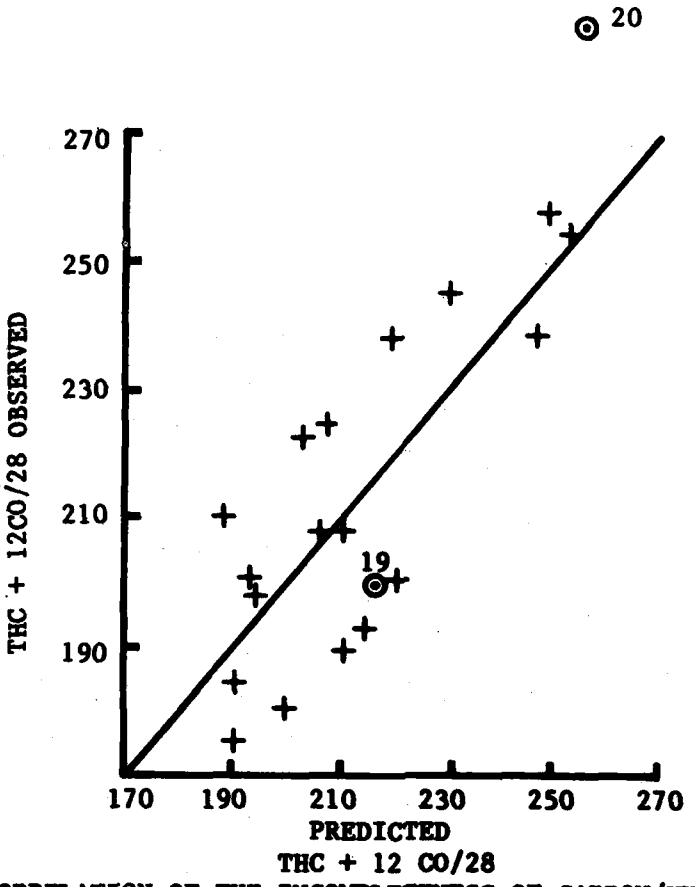

FIGURE 17. CORRELATION OF THE INCOMPLETENESS OF CARBON/HYDROGEN OXIDATION WITH FUEL VISCOSITY AND END POINT; OBSERVED VERSUS PREDICTED VALUES

lar nitrogen, known as the Zeldovich mechanism (16), is important only at high temperatures because the reaction has a very high activation energy (75K cal/mole) and requires a high concentration of oxygen atoms. Oxides of nitrogen originating from fuel-bound nitrogen may form at lower temperatures. Depending on combustor conditions, a significant fraction (75 percent) of the fuel-bound nitrogen may be converted to NO_x. NO_x is formed in the primary zone of the combustor because in that zone the temperatures are the highest, and the fuel oxidation is almost complete. The emissions are highest at high power operating conditions. Except for fuel-bound nitrogen, fuel properties have very little effect on NO_x emissions. Fuel hydrogen content plays a minor role because flame temperature is weakly dependent on H/C ratio.

The NO_x emissions from the test fuels tabulated in Appendix B originated from the oxidation of nitrogen in the air since the fuels contained only negligible amounts of chemically bound nitrogen.

The NO_x emissions indices were essentially the same for all the test fuels, and therefore, showed virtually no effect of fuel properties.

G. Fuel Atomization and Ignition Properties

1. Spray Quality

The fuel spray quality is particularly important for ignition and idle conditions. For ignition, the smallest possible drop sizes are desirable, but the fuel flow rates are low and hence the fuel pressure is low. For pressure atomizing nozzles, the drop sizes increase as the pressure decreases, so atomization at the low fuel pressures used for ignition is critical. This is one reason that a dual orifice nozzle is used in the T-63 engine; the primary nozzle is of low capacity but provides enough pressure differential to get good atomization at low flow rates, while the secondary nozzle provides enough fuel for higher power conditions without tremendous increases in fuel pressure.

The purpose of these measurements was to determine which fuel properties are important for ignition in the T-63 gas turbine engine. Existing ignition models (17) were used to determine the initial set of candidate fuel properties, and the results of this study were then compared with those models.

Drop size distributions were determined using the forward light scattering diffraction instrument manufactured by Malvern Instruments called the Model 2200 Droplet and Spray Particle Sizer. The Rosin-Rammler distribution function fit the observed data well,

$$R = \exp\left(-(d/X)^N\right)$$

where R represents the normalized weight (or volume) above size d. The parameter X gives a measure of (but is larger than) the peak of the weight frequency distribution while the N value indicates the width of the distribution with narrow distributions giving high N values and vice versa. The width of the distribution is important for ignition because the smallest

drops provide the most vapor. However, for this nozzle, the value of N varied only over the range of 2 to 4 with an average of 2.3, so a single parameter called the Sauter mean diameter (SMD), was used to characterize the drop size instead of the two parameters X and N. The SMD is calculated from X and N and represents an average drop size which would have the same surface area and volume as the actual spray. The SMD is the parameter normally used to characterize sprays for ignition studies. The spray characteristics were measured at a distance of 25.4 mm (1 inch) along the nozzle axis away from the face, at a distance of 12.7 mm (0.5 inch) above the nozzle axis. Drop size data were recorded at fuel pressures of 40 psid (differential pressure) (377 kPa) and 50 psid (446 kPa) and flow rates were determined at both conditions. The measured flow rate at ignition was used with these data to compute the SMD at ignition.

A multiple-variable regression analysis computer program was used to predict the mass flow, $\dot{\omega}$, (grams/sec) as a function of the pressure drop across the nozzle, ΔP (psid), the fuel viscosity, ν (cSt), and the specific gravity or density of the fuel, ρ_f (unitless or g/cm^3),

$$\dot{\omega} = 0.7543\ (\Delta P - 32.5)^{0.554}\ \nu^{-0.099}\ \rho_f^{0.778}$$
$$(r^2 = 0.98)$$

The "r^2" is the correlation coefficient where r^2=1 is a perfect fit.

The term 32.5 accounts for the pressure drop across the shutoff valve in the nozzle.

The droplet sizes expressed as SMD(μm) were correlated against several parameters,

$$SMD = 355.0(\Delta P-32.5)^{-0.391}\ \nu^{0.065}\ \rho_f^{1.07}$$
$$(r^2=0.82)$$

or

$$SMD = 293.1\ \dot{\omega}^{-0.714}\ \rho_f^{1.62}$$
$$(r^2=0.85)$$

Trying to predict SMD using both ΔP and $\dot{\omega}$ leads to problems because they are not independent variables; their linear correlation coefficient is 0.98. The resulting equation is

$$SMD = 259.0\ (\Delta P - 32.5)^{0.217}\ \dot{\omega}^{-1.10}\ \nu^{-0.043}\ \rho_f^{1.92}$$
$$(r^2 = 0.86)$$

2. Ignition

Having determined the effect of fuel properties on spray quality and having computed the SMD at the ignition, the effects of droplet size and volatility on ignition were examined. Most of the important ignition data are shown in Table 17. It may be seen from the table and the previous equations for SMD that the drop size for a fixed mass flow rate is fairly constant, with the viscosity variation by a factor of 4 having little effect in this nozzle at a low flow condition. The SMD at the ignition flow rate condition shows a greater variation which is due to the lower flow rates required for ignition with the more volatile fuels and the correspondingly larger SMD's.

These ignition data were first correlated using the model of Ballal and Lefebvre (17) based on the transfer number as given by Spalding. (18) This model has been used to correlate the ignition of fuel drops in quiescent air and in flowing mixtures. According to this model, the minimum ignition energy, E_{min}, required to ignite fuel droplets in quiescent air is

$$E_{min} = \left[\frac{(1/6)\ \pi\ C_{p,a}\ \Delta T_{st}\ (SMD)^3}{\rho_a^{1/2}}\right] \cdot \left[\frac{\rho_f}{\phi\ \ln(1+B)}\right]^{3/2}$$

The parameters that varied in the experiment were Sauter mean diameter, SMD, the equivalence ratio, ϕ, and the mass transfer number, B. The volatility dependence is carried by the transfer number B.

$$B = \frac{q_{st}H + C_{p,a}\ (T_g - T_b)}{L + C_{p,f}\ (T_b - T_s)}$$

TABLE 17. IGNITION DATA

Fuel No.	Fuel/Air Ratio at Ignition,* wt.	T_{inlet}, °C	$T_{10\%\ Pt.}$, °C	SMD 165 grams/min, μm	SMD at Ignition, μm	Viscosity, cP	B	$\frac{(SMD)^2}{q \ln(1+B)} \cdot 10^5$
1	0.0245	36	238	109	68	3.17	3.77	1.3
2	0.0085	26	91	116	161	0.78	7.01	17.0
3	0.0177	26	195	92	81	1.50	4.38	2.3
4	0.0184	29	203	107	90	2.56	4.31	2.9
5	0.0184	29	193	107	89	2.35	4.48	2.7
6	0.0121	29	159	98	112	1.16	5.14	6.0
7	0.0197	27	201	102	84	1.98	4.30	2.3
8	0.0146	28	113	97	100	2.19	6.33	4.4
9	0.0182	28	209	115	92	3.33	4.21	3.2
10	0.0189	28	204	109	92	2.07	4.27	2.9
11	0.0171	26	116	99	93	1.63	6.15	3.2
12	0.0224	31	214	117	69	3.49	4.16	1.5
13	0.0153	27	144	97	96	1.21	5.42	3.6
14	0.0133	31	103	100	105	1.30	6.77	5.1
15	0.0125	31	176	105	121	1.14	4.81	6.9
16	0.0128	26	99	109	121	1.04	6.73	6.7
17	0.0155	31	181	99	97	1.46	4.72	3.7
18	0.0215	28	241	113	72	3.55	3.76	1.7

*F/A Ratio when ignition occurred within 2 seconds after the fuel and igniter were turned on.

where

q_{st} = fuel air ratio for stoichiometric mixture, by mass

H = heat of combustion

$C_{p,a}$ = specific heat at constant pressure, air

$C_{p,f}$ = specific heat at constant pressure, fuel

T_g = gas temperature

T_b = boiling point of fuel

T_s = surface temperature of fuel

L = heat of vaporization

Different authors have started with the above equation but interpreted the terms differently. Spalding (18) is usually quoted in reference to this equation, and the conventions used here follow his examples. Thus, T_g is taken as the inlet air temperature before combustion, and T_s is the initial fuel temperature in the nozzle. Peters and Mellor (19), in particular, have interpreted this equation differently. The boiling point was taken as the 10 percent distillation temperature, as suggested by Peters and Mellor.(19) In order to examine the effects of volatility, a first estimate of B was made by fixing all values in the equation for B except T_g, T_s, and T_b, and using typical values for Jet A fuel for the other parameters. Using q_{st} = 0.068, H = 10325 cal/g, $C_{p,a}$ = 0.240 cal/g °K, $C_{p,f}$ = 0.51 cal/g °K, L = 64.5 cal/g, and $T_g = T_s$ = inlet temperature, the values of B shown in Table 17 were computed.

This experiment was operated with a constant ignition energy, E_{min}, of approximately 300 mJ, and the fuel/air ratio was increased until ignition occurred. According to the equation given above for E_{min}, the quantity $(SMD)^2/\phi \ln(1+B)$ should be approximately constant for all the fuels tested. Also, q was used in place of ϕ, but these are proportional. This correlation was less than adequate to explain the observed variation in fuel/air ratio for ignition. The variation of fuel/ air ratios was a factor of approximately 2.9, while the "constant ratio" $SMD^2/q \ln(1+B)$ varied by a factor of 13!

Why did this model fail? One of the assumptions in the model is that the mixture at the spark plug is composed of fuel drops and air with negligible fuel vapor. The model then assumes a steady-state process of balancing the energy required to heat up and vaporize the fuel drops with that obtained by the energy release in burning the fuel. Perhaps these assumptions are not valid for the T-63 combustor in that the spray may be highly vaporized at the igniter. It is puzzling that Peters and Mellor successfully used a modified version of this model to predict ignition in the T-63 combustor. However, they used a different interpretation of B and also fixed ϕ at a constant value of $\phi = 1.0$.

It was possible to correlate this data by replacing the ln (1+B) term with another term for predicting equilibrium vapor pressures (i.e., the Clausius-Clapeyron equation), so that the constant ratio may be written as

$$SMD^2/qP_v,$$

where the vapor pressure P_v is expressed below

$$P_v = C_1 \exp[C_2/(T_{10\%} - T_{inlet})],$$

The constants C_1 and C_2 were determined by a least-squares analysis and a reasonable correlation coefficient of $r^2 = 0.77$ was obtained. To investigate the importance of the SMD^2 term, the correlation was repeated for the constant term SMD/qP_v and $1/qP_v$. Surprisingly, the correlation coefficient remained about constant, giving no clue as to what power of SMD should be included. The least-squares equations obtained were as follows,

$$\ln (SMD^2/q) = \frac{149.0}{T_{10\%} - T_{inlet}} + 12.0 \qquad (r^2 = 0.77)$$

$$\ln (SMD/q) = \frac{103.5}{T_{10\%} - T_{inlet}} + 7.84 \qquad (r^2 = 0.77)$$

$$\ln (1/q) = \frac{57.89}{T_{10\%} - T_{inlet}} + 3.65 \qquad (r^2 = 0.78)$$

It appears that the fuel/air ratio required for ignition correlates more favorably with the 10-percent distillation point than the drop size. These results suggest that the vapor formed before the mixture reaches the igniter is the significant parameter. Since droplet size depends on viscosity, it appears that this fuel property is less important to ignition than 10 percent point. However, it was not possible to independently vary the fuel/air ratio and the drop size, so their effects are difficult to compare.

V. CONCLUSIONS

A. Diesel Engine Work

- All four engines were successfully modeled using the computer program BMDP1R. Engine load was quantified in terms of energy input, speed, aromatic content, kinematic viscosity, 10%BP, and cetane number.

- The performance of the DD 4-53T engine is adversely affected by highly aromatic fuels. This effect is small, but significant.

- The performance of the Continental Motors LDT-465-1C engine is adversely affected by low 10%BP fuels. This is attributed to the MAN combustion system's dependence on vaporization for combustion. Again, this effect was small but significant.

- The performance of the Cummins NTC-350 engine was not significantly affected by changes in fuel properties over the ranges tested.

- The Caterpillar 3208T engine was operated significantly below its rated power. Results of this investigation should be considered a subset of total engine performance. The 3208T was not significantly affected by changes in fuel properties over the ranges tested.

- The Caterpillar 3208T seemed to produce a higher load per unit of energy consumption than the other engines. This is probably due to its

derated operation. The DD 4-53T was very close to the 3208T followed by the Cummins NTC-350 and the Continental LDT-465-1C.

- The prediction equations cross-correlated quite well, using two fuels that were external to the analysis. This indicates that the equations may be valid for fuels with properties within or close to the test fuels properties.

- Cetane number did not significantly affect the performance of any of the engines. This indicates that test fuel cetane numbers were not low enough to adversely affect combustion at the ambient temperatures encountered in this test.

- Under the operating conditions listed herein and over the range of fuel properties tested, the Cummins NTC-350 and Caterpillar 3208T proved to be more fuel tolerant than either the Detroit Diesel 4-53T or the LDT-465-1C. The adverse effects (loss of power) associated with high aromatics (for the 4-53T) and low 10% BP (for the LDT-465-1C) are small and probably would not be noticed by a vehicle operator.

- Ranking the test fuels proved to be very difficult. Another statistical method would have to be employed to accomplish this.

B. Gas Turbine Combustor Work

- At ignition conditions, the Sauter mean diameter (SMD) of the spray from a T-63 nozzle at the edge of the spray cone and 25.4 mm along the nozzle axis is related to fuel properties by

$$SMD = 355.0\ (\Delta P - 32.5)^{-0.391}\ \mu^{0.065}\ \rho_f^{1.07}$$

Over the range of fuel viscosities tested, the drop size varied only slightly at a given flow rate.

- Ignition models which assume that no fuel is vaporized prior to heat-up by the spark plug are not applicable to the T-63 engine. The ignition data correlate best with a model based on equilibrium values of vapor pressure, where the vapor pressure of the lightest 10 percent fraction is chosen as the correlating parameter.

- The flame radiation and exhaust smoke from the test Fuels 1 through 18 correlated favorably with H/C ratio.

- The radiation and smoke from Fuel 19 were higher and Fuel 20 were lower than the correlation.

- The correlations of THC, CO, and combustion efficiency with viscosity and end point based on Fuels 1 through 18 predicted trends in Fuels 19 and 20 which were not included in the correlations.

- Fuel viscosity had a greater influence than the boiling point distribution on the combustion efficiency and the emissions of THC and CO.

- NO_x emissions were essentially independent of fuel properties.

VI. RECOMMENDATIONS

A. Diesel Engine Work

- Additional tests should be performed to determine the effects of temperature and fuel properties on engine performance and startability.

- Additional tests should be performed to determine the effect of fuel properties on the deliverability of fuels by the fuel systems on these engines. Viscosity and volatility are known to affect deliverability, but to date have not been quantified. Temperature plays an important role in deliverability and should be included in this analysis.

B. Gas Turbine Work

- In the gas turbine studies, additional fuel blends should be prepared that have low viscosities and high end points and vice versa. Generally, fuels that have high viscosity also have high end points. In correlating the total hydrocarbon and CO emissions, it is difficult to discern the relative effects of viscosity and end point when they both follow the same trend. A similar problem was realized in the ignition studies where there naturally exists a strong correlation between viscosity and 10%BP.

VII. LIST OF REFERENCES

1. Olson, D.R., Meckel, N.T. and Quillian, R.D., Jr., "The Operation of Compression-Ignition Engines on Wide Boiling Range Fuels," SAE Transactions, 70, 1962.

2. Hills, F.J. and Schleyerbach, C.G., "Diesel Fuel Properties and Engine Performance," Society of Automotive Engineers, Paper No. 770316, Detroit, MI, 1977.

3. Lestz, S.J., LePera, M.E. and Bowen, T.C., "Fuel and Lubricant Composition Effects on Army Two-Cycle Diesel Engine Performance," Society of Automotive Engineers, Paper No. 760717, Dearborn, MI, 1976.

4. LePera, M.E., "The U.S. Army's Alternative and Synthetic Fuels Program," Army Research, Development, and Acquisition Magazine, 18-20, September-October 1980.

5. Moses, C.A. and Naegeli, D.W., "Fuel Property Effects on Combustor Performance," ASME 79-GT-178 (1979).

6. Naegeli, D.W. and Moses, C.A., "Effects of Fuel Properties on Soot Formation in Turbine Combustion," SAE paper 781026.

7. Blazowski, W.S., "Combustion Considerations for Future Jet Fuels," Sixteenth Symposium (International) on Combustion, MIT, Cambridge, MA, (1976).

8. Lefebvre, A.H., "Progress and Problems in Gas Turbine Combustion," Tenth Symposium (International) on Combustion, University of Cambridge, England (1964).

9. Gleason, C.C. and Martone, J.A., "Fuel Character Effects on J79 and F101 Engine Combustor Emissions," J. Energy, 4 (5), 223 (1980).

10. Shirmer, R.M. and Quigg, H.T., "High Pressure Combustor Studies of Flame Radiation as Related to Hydrocarbon Structure," Phillips Petroleum Company, Report No. 3952-65R.

11. Colket, M.B., Stefucza, J.M., Peters, J.E. and Mellar, A.M., "Radiation and Smoke for Gas Turbine Flames, Part II; Fuel Effects of Performance," Purdue University, Report No. PURDU-CL-77-01.

12. Jackson, T.A. and Blazowski, W.S., "Fuel Hydrogen Content as an Indicator of Radiative Heat Transfer in an Aircraft Gas Turbine Combustor.

13. Friswell, N.J., "The Influence of Fuel Composition on Smoke Emissions from Gas-Turbine-Type Combustors: Effect of Combustor Design and Operating Conditions, "Combustion Science and Technology, 19, 119, 1979.

14. Naegeli, D.W., Fodor, G.E., and Moses, C.A., "Fuel Microemulsions for Jet Engine Smoke Reduction," Report No. ESL-TR-80-25, May 1980.

15. Hardin, M.C., "Calculation of Combustion Efficiency and Fuel/Air Ratio From Exhaust Gas Analysis, "Technical Data Report RN78-48, Detroit Diesel Allison Division, General Motors Corporation, Indianapolis, IN, 27 July 1973.

16. Glassman, I., "Combustion," Academic Press, Inc., 111 Fifth Avenue, New York, NY, 1977.

17. Ballal, D.R. and Lefebvre, A.H., "Ignition and Flame Quenching of Flowing Heterogeneous Fuel-Air Mixtures," Combustion and Flame, Vol. 35, pp 155-168, 1979.

18. Spalding, D.B., Some Fundamentals of Combustion, Butterworths Scientific Publications, London, 1955.

19. Peters, J.E. and Mellor, A.M., "An Ignition Model for Quiescent Fuel Sprays," Combustion and Flame, Vol. 38, pp 65-74, 1980.

APPENDIX A
DETERMINATION OF THE NUMBER OF TEST FIELDS

DETERMINATION OF THE NUMBER OF TEST FUELS

The determination of the appropriate sample size to use in this study is contingent on several factors as will be discussed below. Consider a prediction equation of the form

$$\hat{Y} = \hat{\beta}_0 + \hat{\beta}_1 X_1 + \hat{\beta}_2 X_2 + \hat{\beta}_3 X_3 + \hat{\beta}_4 X_4 + \hat{\beta}_5 X_6, \qquad (1)$$

where

Y = dependent variable (i.e., fuel flow or brake horsepower)
X_1 = cetane number
X_2 = viscosity
X_3 = aromatic content (%)
X_4 = volatility (10% recovered)
X_5 = average volatility (10%-50%-90% recovered)
$\hat{\beta}_j$ = estimated coefficient of X_j, $j = 1, 2, 3, 4, 5$.

Assuming one desires to estimate the regression coefficients, $\hat{\beta}_j$, accurately so that one can effectively evaluate the parameters associated with the prediction of engine performance, it is necessary to specify or estimate the following values:

1. t = value determined from a statistical table by specifying the confidence level, number of independent variables, probability of detecting a specified difference in engine performance and the error degrees of freedom.

2. σ^2 = squared standard deviation in measuring engine performance.

3. $(X_{ii})^{-1}$ = diagonal element of the inverse of the matrix $X'X$ where $X = (\underline{X}_1, \underline{X}_2, \underline{X}_3, \underline{X}_4, \underline{X}_5)$.

4. V_1 = number of independent variables.

5. d = smallest difference in engine performance measurement that is desired to be detected as a significant result.

6. r_i = range of the ith independent variable.

The formula used for determining the sample size, n_i, required for each independent variable is given by (see Wheeler, R.E., Technometrics, 16, 193-202 (1974) termed "Portable Power"):

$$n_i = t^2\sigma^2(X_{ii})^{-1}\, r_i^2(V_1 + 1)d^{-2} \qquad (2)$$

After obtaining n_1, n_2, n_3, n_4, and n_5, the largest value of n_1 is selected as the desired sample size.

In the current study, the values chosen to be inserted in formula (2) are as follows:

1. t = 2.1 (based on a 95 percent confidence level and a 95 percent probability of detecting the difference specified below).

2. σ^2 = 0.50 (based on assuming a 2 percent standard deviation and an average value of brake horsepower of 35., i.e., σ = (0.02)(35) = 0.7.

3. $(X_{ii})^{-1}$ =

$$\begin{cases} 0.00985, & i = 1 \quad \text{(cetane number)} \\ 0.62540, & i = 2 \quad \text{(viscosity)} \\ 0.00000, & i = 3 \quad \text{(aromatic content)} \\ 0.00178, & i = 4 \quad \text{(volatility)} \\ 0.00245, & i = 5 \quad \text{(average volatility)} \end{cases}$$

4. V_1 = 5

5. d =

$$\begin{cases} 6\text{-}16, & \text{for brake horsepower} \\ 3\text{-}7.5, & \text{for fuel flow} \end{cases}$$

6.

$$r_i = \begin{cases} 32, & i = 1 \quad \text{(cetane no. 23-55)} \\ 4.3, & i = 2 \quad \text{(viscosity 0.7-5.0)} \\ 40, & i = 3 \quad \text{(aromatic content 10-50} \\ 149, & i = 4 \quad \text{(volatility-10\% 90-239)} \\ 132, & i = 5 \quad \text{(average volatility-10\%-50\%-90\% 140-272)} \end{cases}$$

Employing the above values, we find that

$$(X_{ii})^{-1} r_i^2 = \begin{cases} 10.09, & i = 1 \\ 11.56, & i = 2 \\ 0.001, & i = 3 \\ 39.54, & i = 4 \\ 42.69, & i = 5 \end{cases}$$

Hence, the largest n_i will be n_5 and will be given by equation (2), i.e.,

$$n_5 = t^2\sigma^2 (X_{ii})^{-1} r_i^2 (V_1 + 1)d^{-2}$$

$$= (256.13)(t^2\sigma^2 d^{-2})$$

The values of t, σ, and d will control the size of the sample. If $\sigma = 0.71$, and $d = 6$, then $t = 2.1$ and the sample size should exceed

$$n = (256.13)\ (2.1)^2 (0.7)^2 (6)^{-2}$$
$$= 15.37$$

Therefore, the sample size required is 16 or more observations.

It should be noted that other choices of σ or d will yield larger or smaller sample sizes.

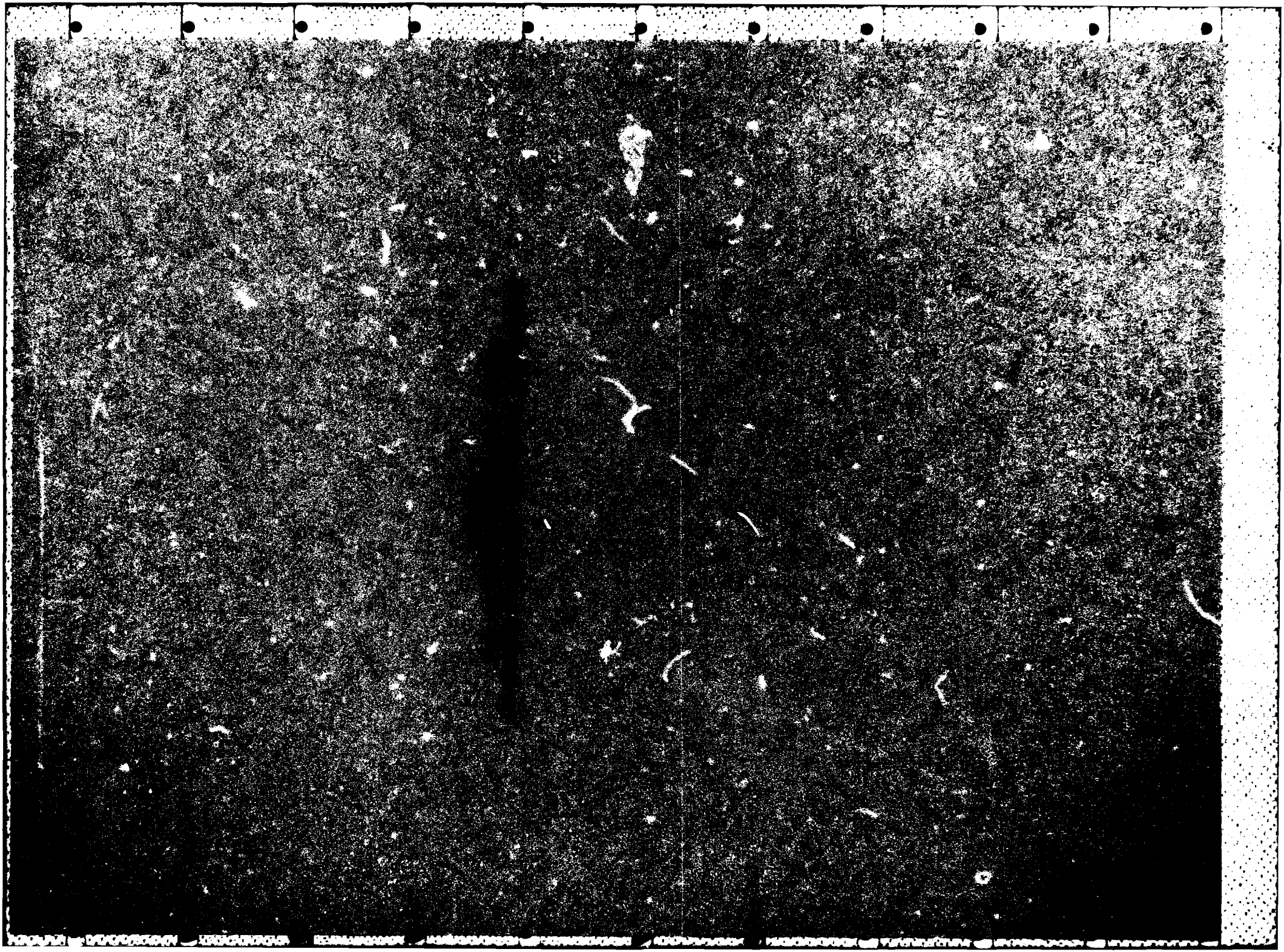

FUEL PROPERTIES CORRELATION MATRIX

		API Gravity 1	Specific Gravity 2	Distillation, °C: IBP 3	10% recovered 4	50% recovered 5	90% recovered 6	EP 7	Residual 8	Loss 9	Viscosity @ 40°C 10	Aromatics 11	Olefins 12	Mono-Aromatics 13	Di-Aromatics 14
API Gravity	1	1.0000													
Sp. Gr., g/ml	2	-0.8254	1.0000												
Distillation, °C															
IBP	3	-0.8074	0.5794	1.0000											
10% recovered	4	-0.8390	0.6302	0.9477	1.0000										
50% recovered	5	-0.8190	0.6576	0.5385	0.6283	1.0000									
90% recovered	6	-0.5507	0.5318	0.2404	0.2625	0.8171	1.0000								
EP	7	-0.5455	0.5321	0.2099	0.2367	0.8085	0.9945	1.0000							
Residual	8	-0.1250	0.1340	0.1047	0.0577	0.3704	0.6512	0.6392	1.0000						
Loss	9	-0.2284	0.2254	-0.0911	0.0182	0.3425	0.3140	0.3183	-0.0687	1.0000					
Viscosity @ 40°C	10	-0.7918	0.7194	0.6632	0.7418	0.9117	0.7846	0.7625	0.4941	0.1544	1.0000				
Aromatics	11	-0.8807	0.7891	0.6178	0.5996	0.5792	0.4018	0.4150	0.0358	0.1443	0.5313	1.0000			
Olefins	12	-0.4286	0.4432	0.3766	0.3518	0.1529	0.0330	0.0138	-0.1940	-0.0159	0.2157	0.5995	1.0000		
Mono-Aromatics	13	-0.3370	0.3576	0.2868	0.1466	-0.1368	-0.2553	-0.2401	-0.3735	-0.0922	-0.1830	0.6578	0.5136	1.0000	
Di-Aromatics	14	-0.7859	0.7967	0.4717	0.5875	0.6943	0.5573	0.5697	0.1861	0.2614	0.6948	0.6673	0.2645	0.0531	1.0000
Tri-Aromatics	15	-0.6893	0.6959	0.3621	0.4618	0.9083	0.9058	0.9020	0.5052	0.3276	0.8954	0.4741	0.0604	-0.2561	0.7827
Hydrogen	16	0.9228	-0.8523	-0.6950	-0.6966	-0.9552	-0.9539	-0.9413	0.0539	-0.1937	-0.9637	-0.9631	-0.5471	-0.6225	-0.7560
Carbon	17	-0.8117	0.7083	0.6374	0.5842	0.4004	0.2119	0.2141	-0.0778	0.0024	0.3848	0.9456	0.5788	0.7577	0.6016
Nitrogen	18	-0.3646	0.3802	0.2218	0.2197	0.3372	0.3484	0.3300	0.2665	-0.1213	0.4111	0.5298	0.7140	0.2393	0.2604
Sulfur	19	-0.7009	0.7164	0.3859	0.5074	0.7804	0.7093	0.7189	0.3100	0.3063	0.7686	0.4783	0.0571	-0.1762	0.9265
Refractive Index @ 20°C	20	-0.9813	0.8865	0.7373	0.7665	0.7788	0.5621	0.5600	0.1362	0.2220	0.7653	0.9182	0.4726	0.3945	0.8427
Carbon Residue, 10% Btms	21	-0.4754	0.4877	0.3349	0.4016	0.5700	0.6560	0.6562	0.6951	0.3353	0.6423	0.3217	0.0256	-0.2579	0.6100
Aniline Point	22	0.1373	-0.1881	-0.0880	0.0182	0.3741	0.4635	0.4367	0.5152	0.0858	0.4188	-0.4944	-0.4323	-0.9164	-0.0233
Flash Point	23	-0.8511	0.6327	0.9886	0.9666	0.5909	0.2866	0.2550	0.0810	-0.0078	0.6980	0.6629	0.4214	0.2844	0.5138
Net Heat of Combustion	24	0.8273	-0.6102	-0.6528	-0.6561	-0.3957	-0.3479	-0.3491	-0.0555	-0.2309	-0.5631	-0.7734	-0.4116	-0.3730	-0.7255
Calculated Net Heat of Combustion	25	0.8716	-0.7711	-0.6892	-0.6733	-0.4770	-0.1935	-0.2038	0.1937	-0.1406	-0.4327	-0.9365	-0.5440	-0.7146	-0.6622
Cetane No.	26	-0.1866	0.0240	0.1869	0.3328	0.6059	0.5125	0.4904	0.3392	0.1835	0.6092	-0.2394	-0.3471	-0.8033	0.2305
Cetane Index	27	0.0544	-0.1799	-0.2897	-0.1637	-0.4972	0.5821	0.5853	0.4196	0.2680	0.3407	-0.2933	-0.4235	-0.7762	0.0672

		Tri-Aromatics 15	Hydrogen 16	Carbon 17	Nitrogen 18	Sulfur 19	Refractive Index @ 20°C 20	Carbon Residue 10% Btms 21	Aniline Point 22	Flash Point 23	Net Heat of Combustion 24	Calculated Net Heat of Combustion 25	Cetane No. 26	Cetane Index 27
Tri-Aromatics	15	1.0000												
Hydrogen	16	-0.5062	1.0000											
Carbon	17	0.3004	-0.9380	1.0000										
Nitrogen	18	0.3003	-0.3884	0.4141	1.0000									
Sulfur	19	0.9007	-0.5848	0.3792	0.1338	1.0000								
Refractive Index @ 20°C	20	0.7086	-0.9564	0.8575	0.4179	0.7359	1.0000							
Carbon Residue, 10% Btms	21	0.6722	-0.3328	0.1851	0.1627	0.6536	0.4877	1.0000						
Aniline Point	22	0.4304	0.4740	-0.6378	-0.0814	0.2621	-0.2155	0.3684	1.0000					
Flash Point	23	0.4099	-0.7354	0.6630	0.2549	0.4204	0.7822	0.3640	-0.0851	1.0000				
Net Heat of Combustion	24	-0.4867	0.8161	-0.7737	-0.3965	-0.6101	-0.8359	-0.3790	0.2523	-0.6553	1.0000			
Calculated Net Heat of Combustion	25	-0.3497	0.9786	-0.9551	-0.3066	-0.4637	-0.8961	-0.1791	0.5966	-0.7208	0.7961	1.0000		
Cetane No.	26	0.5904	0.1647	-0.3905	-0.1082	0.4757	0.0826	0.3637	0.8974	0.2079	0.0103	0.2737	1.0000	
Cetane Index	27	0.5145	0.3413	-0.4907	-0.0359	0.3164	-0.1135	0.2817	0.8290	-0.2545	0.1811	0.4552	0.7904	1.0000

TURBINE COMBUSTION PERFORMANCE MEASUREMENTS

Fuel No.	EXHAUST SMOKE NUMBER: SN 10% Power	SN 55% Power	SN 75% Power	SN 100% Power		FLAME RADIATION, kW/m²: 10% Power Radiation	55% Power Radiation	75% Power Radiation	100% Power Radiation		TOTAL HYDROCARBON EMISSIONS INDEX: 10% Power THC E.I.	55% Power THC E.I.	75% Power THC E.I.	100% Power THC E.I.
					H									
Ref.	6.3	9.0	10.8	15.5	14.15	24.5	54.1	69	102.2	1.964	140.0	21.6	7.5	3.5
1	27	16.1	22.4	25.7	12.95	44.7	87.8	115.5	135	1.789	176.3	23.3	11.1	4.2
2	5.0	8.3	13.8	15.2	14.34	25.4	51.3	68.9	99.7	1.995	134.6	19.4	7.3	3.7
3	11.0	11.9	16.6	19.5	13.7	28.4	63.4	78.1	117.5	1.901	153.1	25.4	9.6	4.6
4	22	21.4	25.6	27.1	12.89	44.0	98.1	100.5	156.4	1.784	131.1	21.6	10.6	7.0
5	27	26.2	31.2	29.8	12.53	50.7	98.8	105.8	169.3	1.725	126.1	22.6	11.6	9.1
6	7.9	12.0	14.6	16.3	14.06	25.4	45.3	72.1	103.8	1.956	128.3	20.3	7.8	14
7	18.0	14.6	19.3	20.4	13.54	34.4	69.2	92.8	120.4	1.866	165.2	24.4	11.1	4.6
8	16	13.6	16.3	19.0	13.66	30.6	61.7	85.2	125.4	1.896	148.2	23.9	12.0	5.6
9	14	14.3	16.9	22.7	13.51	34.4	68.0	115.0	128.4	1.866	187.2	21.8	7.6	12.4
10	40	26.4	32.2	44.6	12.05	66.3	102.8	129	214.1	1.635	159.8	20.2	13.5	5.6
11	19	12.7	18.5	19.0	13.6	32.9	65.5	89.8	118.9	1.880	167.5	27.4	11.0	4.6
12	30	25.6	33.3	37.3	12.33	59.6	119.1	151.7	201.6	1.680	177.2	32.8	11.0	4.1
13	12	11.0	13.6	15.3	14.0	27.7	51.8	80.2	111.6	1.938	151.0	27.5	8.9	3.7
14	6	8.2	13.9	17.1	14.05	24.0	57.8	77.4	112.9	1.945	179.7	26.6	9.8	5.0
15	27	22.8	28.7	31.4	12.73	44.0	100.8	132.3	184.7	1.740	143.3	26.4	8.0	4.8
16	13.2	11.6	14.4	16.8	13.93	28.4	55.1	85.9	110.0	1.915	155.0	28.5	8.7	4.5
17	19	18.7	24.0	30.0	13.12	34.4	89.8	117.5	162.2	1.803	135.0	26.4	7.3	4.3
18	21	16.2	21.5	26.5	13.04	38.8	92.6	111.6	156.2	1.798	186.9	25.8	8.0	3.9
19	11.5	17.6	21.5	27.9	13.45	33.9	87.8	117.5	174.4	1.853	160.6	22.2	7.9	4.4
20	49	29.7	38.3	57.4	10.57	99.1	181.3	225.9	280.0	1.429	198.2	27.3	13.0	4.8

Fuel No.	CARBON MONOXIDE EMISSIONS INDEX: Power 10%	55%	75%	100%	COMBUSTION EFFICIENCY: Power 10%	55%	75%	100%	NITROGEN OXIDES EMISSIONS INDEX: 10%	55%	75%	Power 100%
Ref.	117.0	45.8	27.8	13.0	94.9	98.5	99.3	99.7	2.5	4.3	5.0	6.7
1	161.0	57.2	33.6	16.2	92.8	98.3	99.0	99.5	2.5	4.2	4.9	6.1
2	107.1	44.5	25.3	11.6	94.6	98.6	99.3	99.6	2.8	4.6	5.2	6.9
3	133.0	55.1	31.4	14.3	94.0	98.3	99.1	99.6	2.8	4.6	5.2	6.9
4	144.9	54.1	35.1	15.8	94.6	98.3	99.0	99.5	2.5	4.0	5.3	6.8
5	148.3	57.3	36.1	16.7	94.5	98.1	99.0	99.5	2.4	3.9	4.9	6.9
6	109.8	44.3	28.4	12.3	95.5	98.6	99.3	99.4	2.6	4.1	5.8	7.9
7	134.2	53.6	31.5	13.9	93.5	98.3	99.0	99.6	2.5	4.2	4.8	6.4
8	122.2	58.2	36.7	16.9	94.6	98.0	99.0	99.5	2.5	4.1	5.5	7.4
9	120.9	56.6	37.0	16.8	94.2	98.2	99.1	99.4	2.4	4.2	5.1	7.6
10	112.8	56.7	40.6	17.6	94.6	98.3	98.9	99.5	2.7	4.3	5.0	7.3
11	133.9	56.9	33.5	14.5	93.4	98.2	99.0	99.6	2.5	4.1	5.0	6.1
12	180.5	59.8	39.9	14.5	93.2	98.1	98.9	99.6	2.3	4.6	5.4	6.4
13	116.7	48.6	31.0	13.3	94.3	98.5	99.1	99.6	2.7	4.3	5.2	5.9
14	136.3	50.7	34.9	12.7	93.6	98.4	99.1	99.6	2.4	4.7	5.5	7.0
15	128.5	47.8	33.5	12.6	95.0	98.6	99.2	99.6	2.8	4.6	5.6	7.0
16	124.6	53.2	30.1	13.3	93.9	98.4	99.2	99.6	2.7	4.4	5.0	6.0
17	115.9	47.1	33.9	11.5	95.5	98.7	99.2	99.7	2.7	4.0	5.5	6.8
18	165.1	49.3	33.1	11.6	94.1	98.6	99.2	99.7	2.5	4.6	5.4	6.5
19	132.6	46.8	29.4	13.9	94.3	98.3	99.3	99.5	2.8	4.5	5.4	6.7
20	212.7	81.7	41.9	22.4	92.3	97.3	98.8	99.3	3.6	4.7	5.5	6.3

LIST OF ACRONYMS AND ABBREVIATIONS

BP	Boiling Point
BTX	Benzene, toluene, xylene
CC	Correlation coefficient
CI	Compression ignition
CN	Cetane Number
COED	Computer-Optimized Experimental Design
CO_x	Carbon oxides
DD	Detroit Diesel
ϵ	Combustion efficiency
ED	End point
FIA	Fluorescent Indicator Adsorption
HAN	High Aromatic Naphtha
H/C Ratio	Ratio of hydrogen to carbon atoms
LDT-465-1C	Continental Motors engine designation
MAN	Combustion system developed by Maschinenfabrik Augsburg-Nürnberg AG
NO_x	Nitrous Oxides
NTC	Cummins Engine Company engine designation
R	Radiation
Residual	Predicted value-observed value
SI	Spark ignition
SMD	Sauter Mean Diameter
T	Standard statistical method for expressing significance of a coefficient
THC	Total hydrocarbons
USAFLRL	U.S. Army Fuels and Lubricants Research Laboratory
USAMERADCOM	U.S. Army Mobility Equipment Research and Development Command
V	Viscosity
VF	Viscosity Blending Index Factor

DISTRIBUTION LIST

DEPARTMENT OF DEFENSE

DEFENSE DOCUMENTATION CTR
CAMERON STATION 12
ALEXANDRIA VA 22314

DEPT OF DEFENSE
ATTN: DASD(MRAL)-LM(MR DYCKMAN) 1
WASHINGTON DC 20301

COMMANDER
DEFENSE LOGISTICS AGY
ATTN DLA-SME (MRS P MCLAIN) 1
CAMERON STATION
ALEXANDRIA VA 22314

COMMANDER
DEFENSE FUEL SUPPLY CTR
ATTN: DFSC-T (MR. MARTIN) 1
CAMERON STA
ALEXANDRIA VA 22314

COMMANDER
DEFENSE GENERAL SUPPLY CTR
ATTN: DGSC-SSA 1
RICHMOND VA 23297

DOD
ATTN: DUSC (RAT) (Dr. Dix) 1
ATTN: DUSD (RTI) (Dr. Young) 1
WASHINGTON, DC 20301

DOD
ATTN OASD (MRA&L)-TD 1
PENTAGON, 3C841
WASHINGTON DC 20301

DEFENSE ADVANCED RES PROJ AGENCY
DEFENSE SCIENCES OFC 1
1400 WILSON BLVD
ARLINGTON VA 22209

DEPARTMENT OF THE ARMY

HQ, DEPT OF ARMY
ATTN: DALO-TSE (COL ST.ARNAUD) 1
DALO-AV 1
DALO-SMZ-E 1
DAMA-CSS-P (DR BRYANT) 1
DAMA-ARZ (DR CHURCH) 1
WASHINGTON DC 20310

CDR
U.S. ARMY MOBILITY EQUIPMENT
R&D COMMAND
Attn: DRDME-GL 10
DRDME-WC 2
FORT BELVOIR VA 22060

CDR
US ARMY MATERIEL DEVEL&READINESS
COMMAND
ATTN: DRCLD (MR BENDER) 1
DRCDMR (MR GREINER) 1
DRCDMD-ST (DR HALEY) 1
DRCQA-E 1
DRCDE-SG 1
DRCIS-C (LTC CROW) 1
DRCSM-P 1
5001 EISENHOWER AVE
ALEXANDRIA VA 22333

CDR
US ARMY TANK-AUTOMOTIVE CMD
ATTN DRSTA-NW (TWVMO) 1
DRSTA-RG (MR HAMPARIAN) 1
DRSTA-NS (DR PETRICK) 1
DRSTA-G 1
DRSTA-M 1
DRSTA-GBP (MR MCCARTNEY) 1
WARREN MI 48090

DIRECTOR
US ARMY MATERIEL SYSTEMS
ANALYSIS AGENCY
ATTN DRXSY-CM 1
DRXSY-S 1
DRXSY-L 1
ABERDEEN PROVING GROUND MD 21005

DIRECTOR
APPLIED TECHNOLOGY LAB
U.S. ARMY R&T LAB (AVRADCOM)
ATTN DAVDL-ATL-ATP (MR MORROW) 1
DAVDL-ATL-ASV (MR CARPER) 1
FORT EUSTIS VA 23604

HQ, 172D INFANTRY BRIGADE (ALASKA)
ATTN AFZT-DI-L 1
AFZT-DI-M 1
DIRECTORATE OF INDUSTRIAL
OPERATIONS
FT RICHARDSON AK 99505

CDR
US ARMY GENERAL MATERIAL &
PETROLEUM ACTIVITY
ATTN STSGP-F (MR SPRIGGS) 1
STSGP-PE (MR MCKNIGHT),
BLDG 85-3 1
STSGP (COL CLIFTON) 1
NEW CUMBERLAND ARMY DEPOT
NEW CUMBERLAND PA 17070

CDR
US ARMY MATERIEL ARMAMEMT
READINESS CMD
ATTN DRSAR-LEM 1
ROCK ISLAND ARSENAL IL 61299

CDR
US ARMY COLD REGION TEST CENTER
ATTN STECR-TA 1
APO SEATTLE 98733

HQ, DEPT. OF ARMY
ATTN: DAEN-RDZ-B 1
WASHINGTON, DC 20310

CDR
US ARMY RES & STDZN GROUP
(EUROPE)
ATTN DRXSN-UK-RA 1
BOX 65
FPO NEW YORK 09510

HQ, US ARMY AVIATION R&D CMD
ATTN DRDAV-GT (MR R LEWIS) 1
DRDAV-D (MR CRAWFORD) 1
DRDAV-N (MR BORGMAN) 1
DRDAV-E 1
4300 GOODFELLOW BLVD
ST LOUIS MO 63120

CDR
US ARMY FORCES COMMAND
ATTN AFLG-REG 1
AFLG-POP 1
FORT MCPHERSON GA 30330

CDR
US ARMY ABERDEEN PROVING GROUND
ATTN: STEAP-MT 1
STEAP-MT-U (MR DEAVER) 1
ABERDEEN PROVING GROUND MD 21005

CDR
US ARMY YUMA PROVING GROUND
ATTN STEYP-MT (MR DOEBBLER) 1
YUMA AZ 85364

PROJ MGR, ABRAMS TANK SYS
ATTN DRCPM-GCM-S 1
WARREN MI 48090

PROG MGR, FIGHTING VEHICLE SYS
ATTN DRCPM-FVS-SE 1
WARREN MI 48090

PROJ MGR, M60 TANK DEVELOPMENT
USMC-LNO, MAJ. VARELLA 1
US ARMY TANK-AUTOMOTIVE CMD (TACOM)
WARREN MI 48090

PROG MGR, M113/M113A1 FAMILY
VEHICLES
ATTN DRCPM-M113 1
WARREN MI 48090

PROJ MGR, MOBILE ELECTRIC POWER
ATTN DRCPM-MEP-TM 1
7500 BACKLICK ROAD
SPRINGFIELD VA 22150

PROJ MGR, IMPROVED TOW
VEHICLE
US ARMY TANK-AUTOMOTIVE CMD
ATTN DRCPM-ITV-T 1
WARREN MI 48090

CDR
US ARMY EUROPE & SEVENTH ARMY
ATTN AEAGC-FMD 1
ATTN: AEAGC-TE 1
APO NY 09403

PROJ MGR, PATRIOT PROJ OFC
ATTN DRCPM-MD-T-G 1
US ARMY DARCOM
REDSTONE ARSENAL AL 35809

CDR
THEATER ARMY MATERIAL MGMT
CENTER (200TH)
DIRECTORATE FOR PETROL MGMT
ATTN AEAGD-MM-PT-Q 1
ZWEIBRUCKEN
APO NY 09052

CDR
US ARMY RESEARCH OFC
ATTN DRXRO-ZC 1
DRXRO-EG (DR SINGLETON) 1
DRXRO-CB (DR GHIRARDELLI) 1
P O BOX 12211
RSCH TRIANGLE PARK NC 27709

DIR
US ARMY AVIATION R&T LAB (AVRADCOM)
ATTN DAVDL-AS (MR D WILSTEAD) 1
NASA/AMES RSCH CTR
MAIL STP 207-5
MOFFIT FIELD CA 94035

CDR
TOBYHANNA ARMY DEPOT
ATTN SDSTO-TP-S 1
TOBYHANNA PA 18466

DIR
US ARMY MATERIALS & MECHANICS
RSCH CTR
ATTN DRXMR-E 1
DRXMR-R 1
DRXMR-T 1
WATERTOWN MA 02172

CDR
US ARMY DEPOT SYSTEMS CMD
ATTN DRSDS 1
CHAMBERSBURG PA 17201

CDR
US ARMY WATERVLIET ARSENAL
ATTN SARWY-RDD 1
WATERVLIET NY 12189

CDR
US ARMY LEA
ATTN DALO-LEP 1
NEW CUMBERLAND ARMY DEPOT
NEW CUMBERLAND PA 17070

CDR
US ARMY GENERAL MATERIAL &
PETROLEUM ACTIVITY
ATTN STSGP-PW (MR PRICE) 1
SHARPE ARMY DEPOT
LATHROP CA 95330

CDR
US ARMY FOREIGN SCIENCE & TECH
CENTER
ATTN DRXST-MT1 1
FEDERAL BLDG
CHARLOTTESVILLE VA 22901

CDR
DARCOM MATERIEL READINESS
SUPPORT ACTIVITY (MRSA)
ATTN DRXMD-MD 1
LEXINGTON KY 40511

HQ, US ARMY T&E COMMAND
ATTN DRSTE-TO-O 1
ABERDEEN PROVING GROUND, MD 21005

HQ, US ARMY ARMAMENT R&D CMD
ATTN DRDAR-LC 1
DRDAR-SC 1
DRDAR-AC 1
DRDAR-QA 1
DOVER NJ 07801

HQ, US ARMY TROOP SUPPORT &
AVIATION MATERIAL READINESS
COMMAND
ATTN DRSTS-MEG (2) 1
DRCPO-PDE (LTC FOSTER) 1
4300 GOODFELLOW BLVD
ST LOUIS MO 63120

DEPARTMENT OF THE ARMY
CONSTRUCTION ENG RSCH LAB
ATTN CERL-EM 1
CERL-ZT 1
CERL-EH 1
P O BOX 4005
CHAMPAIGN IL 61820

DIR
US ARMY ARMAMENT R&D CMD
BALLISTIC RESEARCH LAB
ATTN DRDAR-BLV 1
DRDAR-BLP 1
ABERDEEN PROVING GROUND, MD 21005

HQ
US ARMY TRAINING & DOCTRINE CMD
ATTN ATCD-S (LTC LESKO) 1
FORT MONROE VA 23651

DIRECTOR
US ARMY RSCH & TECH LAB (AVRADCOM)
PROPULSION LABORATORY
ATTN DAVDL-PL-D (MR ACURIO) 1
21000 BROOKPARK ROAD
CLEVELAND OH 44135

CDR
US ARMY NATICK RES & DEV
ATTN DRDNA-YEP (DR KAPLAN) 1
NATICK MA 01760

CDR
US ARMY TRANSPORTATION SCHOOL
ATTN ATSP-CD-MS 1
FORT EUSTIS VA 23604

CDR
US ARMY QUARTERMASTER SCHOOL
ATTN ATSM-CD (COL VOLPE) 1
ATSM-CDM 1
ATSM-TNG-PT 1
FORT LEE VA 23801

HQ, US ARMY ARMOR CENTER
ATTN ATZK-CD-SB 1
FORT KNOX KY 40121

CDR
101ST AIRBORNE DIV (AASLT)
ATTN: AFZB-KE-J 1
AFZB-KE-DMMC 1
FORT CAMPBELL, KY 42223

CDR
US ARMY LOGISTICS CTR
ATTN ATCL-MS (MR A MARSHALL) 1
FORT LEE VA 23801

CDR
US ARMY FIELD ARTILLERY SCHOOL
ATTN ATSF-CD 1
FORT SILL OK 73503

CDR
US ARMY ORDNANCE CTR & SCHOOL
ATTN ATSL-CTD-MS 1
ABERDEEN PROVING GROUND MD 21005

CDR
US ARMY ENGINEER SCHOOL
ATTN ATSE-CDM 1
FORT BELVOIR VA 22060

CDR
US ARMY INFANTRY SCHOOL
ATTN ATSH-CD-MS-M 1
FORT BENNING GA 31905

CDR
US ARMY AVIATION BOARD
ATTN ATZQ-OT-C 1
ATZQ-OT-A 1
FORT RUCKER AL 36362

CDR
US ARMY MISSILE CMD
ATTN DRSMI-O 1
DRSMI-RK 1
DRSMI-D 1
REDSTONE ARSENAL, AL 35809

CRD
US ARMY AVIATION CTR & FT RUCKER
ATTN ATZQ-D 1
FORT RUCKER AL 36362

PROJ MGR M60 TANK DEVELOP.
ATTN DRCPM-M60-E 1
WARREN MI 48090

CDR
US ARMY INFANTRY BOARD
ATTN ATZB-IB-PR-T 1
FORT BENNING, GA 31905

CDR
US ARMY FIELD ARTILLERY BOARD
ATTN ATZR-BDPR 1
FORT SILL OK 73503

CDR
US ARMY ARMOR & ENGINEER BOARD
ATTN ATZK-AE-PD 1
ATZK-AE-CV 1
FORT KNOX, KY 40121

CDR
US ARMY CHEMICAL SCHOOL
ATTN ATZN-CM-CS 1
FORT MCCLELLAN, AL 36205

DEPARTMENT OF THE NAVY

CDR
NAVAL AIR PROPULSION CENTER
ATTN PE-71 (MR WAGNER) 1
PE-72 (MR D'ORAZIO) 1
P O BOX 7176
TRENTON NJ 06828

CDR
NAVAL SEA SYSTEMS CMD
CODE 05D4 (MR R LAYNE) 1
WASHINGTON DC 20362

CDR
DAVID TAYLOR NAVAL SHIP R&D CTR
CODE 2830 (MR G BOSMAJIAN) 1
CODE 2831 1
CODE 2832
ANNAPOLIS MD 21402

JOINT OIL ANALYSIS PROGRAM -
TECHNICAL SUPPORT CTR 1
BLDG 780
NAVAL AIR STATION
PENSACOLA FL 32508

DEPARTMENT OF THE NAVY
HQ, US MARINE CORPS
ATTN LPP (MAJ SANDBERG) 1
LMM/3 (MAJ STROCK) 1
WASHINGTON DC 20380

CDR
NAVAL AIR SYSTEMS CMD
ATTN CODE 5304C1 (MR WEINBURG) 1
CODE 53645 (MR MEARNS) 1
WASHINGTON DC 20361

CDR
NAVAL AIR DEVELOPMENT CTR
ATTN CODE 60612 (MR L STALLINGS) 1
WARMINSTER PA 18974

CDR
NAVAL RESEARCH LABORATORY
ATTN CODE 6170 (MR H RAVNER) 1
CODE 6180 1
CODE 6110 (DR HARVEY) 1
WASHINGTON DC 20375

CDR
NAVAL FACILITIES ENGR CTR
ATTN CODE 120 (MR R BURRIS) 1
CODE 120B (MR BUSCHELMAN) 1
200 STOVWALL ST
ALEXANDRIA VA 22322

CHIEF OF NAVAL RESEARCH
ATTN CODE 473 1
ARLINGTON VA 22217

CDR
NAVAL AIR ENGR CENTER
ATTN CODE 92727 1
LAKEHURST NJ 08733

COMMANDING GENERAL
US MARINE CORPS DEVELOPMENT
& EDUCATION COMMAND
ATTN: DO75 (LTC KERR) 1
QUANTICO, VA 22134

CDR, NAVAL MATERIEL COMMAND
ATTN MAT-083 (DR A ROBERTS) 1
MAT-08E (MR ZIEM) 1
CP6, RM 606
WASHINGTON DC 20360

CDR
NAVY PETROLEUM OFC
ATTN CODE 40 1
CAMERON STATION
ALEXANDRIA VA 22314

CDR
MARINE CORPS LOGISTICS SUPPORT
BASE ATLANTIC
ATTN CODE P841 1
ALBANY GA 31704

DEPARTMENT OF THE AIR FORCE

HQ, USAF
ATTN LEYSF (MAJ LENZ) 1
WASHINGTON DC 20330

HQ AIR FORCE SYSTEMS CMD
ATTN AFSC/DLF (LTC RADLOFF) 1
ANDREWS AFB MD 20334

CDR
US AIR FORCE WRIGHT AERONAUTICAL
LAB
ATTN AFWAL/POSF (MR CHURCHILL) 1
AFWAL/POSL (MR JONES) 1
AFWAL/MLSE (MR MORRIS) 1
AFWAL-MLBT 1
WRIGHT-PATTERSON AFB OH 45433

CDR
SAN ANTONIO AIR LOGISTICS
CTR
ATTN SAALC/SFQ (MR MAKRIS) 1
SAALC/MMPRR 1
KELLY AIR FORCE BASE, TX 78241

CDR
WARNER ROBINS AIR LOGISTIC
CTR
ATTN WR-ALC/MMIRAB-1 (MR GRAHAM) 1
ROBINS AFB GA 31098

OTHER GOVERNMENT AGENCIES

US DEPARTMENT OF TRANSPORTATION
ATTN AIRCRAFT DESIGN CRITERIA
BRANCH 2
FEDERAL AVIATION ADMIN
2100 2ND ST SW
WASHINGTON DC 20590

DIRECTOR
NATL MAINTENANCE TECH SUPPORT
CTR 2
US POSTAL SERVICE
NORMAN OK 73069

NATIONAL AERONAUTICS AND
SPACE ADMINISTRATION
LEWIS RESEARCH CENTER
MAIL STOP 5420
(ATTN: MR. GROBMAN) 1
CLEVELAND, OH 44135

NATIONAL AERONAUTICS AND
SPACE ADMINISTRATION
VEHICLE SYSTEMS AND ALTERNATE
FUELS PROJECT OFFICE
ATTN: MR. CLARK 1
LEWIS RESEARCH CENTER
CLEVELAND, OH 44135

US DEPARTMENT OF ENERGY
SYSTEMS EEF, ATTN: MR. ALPAUGH 1
1000 INDEPENDENCE AVE., SW
WASHINGTON, DC 20585

DEPARTMENT OF TRANSPORTATION
FEDERAL AVIATION ADMINISTRATION
AWS-110, ATTN: MR. NUGENT 1
800 INDEPENDENCE AVE, SW
WASHINGTON, DC 20590

US DEPARTMENT OF ENERGY
CE-1312, ATTN: MR ECKLUND 1
1000 INDEPENDENCE AVE, SW
WASHINGTON, DC 20585

US DEPARTMENT OF ENERGY
BARTLESVILLE ENERGY RSCH CTR
DIV OF PROCESSING & THERMO RES 1
DIV OF UTILIZATION RES 1
BOX 1398
BARTLESVILLE OK 74003

SCI & TECH INFO FACILITY
ATTN NASA REP (SAK/DL) 1
P O BOX 8757
BALTIMORE/WASH INT AIRPORT MD 21240

ENVIRONMENTAL PROTECTION AGCY
OFFICE OF MOBILE SOURCES
MAIL CODE ANR-455
(MR. G. KITTREDGE) 1
401 M ST. SW
WASHINGTON DC 20460